PHILOSOPHICAL TRANSACTIONS OF THE ROYAL SOCIETY A MATHEMATICAL, PHYSICAL & ENGINEERING SCIENCES

The Stability of Axisymmetric Menisci

J. F. Padday and A. R. Pitt

Phil. Trans. R. Soc. Lond. A 1973 **275**, 489-528
doi: 10.1098/rsta.1973.0113

THE STABILITY OF AXISYMMETRIC MENISCI

By J. F. PADDAY AND A. R. PITT
Research Division, Kodak Limited, Wealdstone, Harrow, Middlesex, HA1 4TY

(*Communicated by D. Tabor, F.R.S.* – *Received* 25 *June* 1973)

CONTENTS

This study is dedicated to the memory of J. Plateau whose stability criteria for soap films (Plateau 1873) was published exactly a century ago.

Vol. 275. A 1253. 41 [Published 31 December 1973

The conditions that govern the equilibrium and stability of a meniscus have been obtained from the first and second derivatives of the energy of the meniscus when it undergoes axisymmetric deformation.

The energy of forming a meniscus is defined in thermodynamic terms and methods are given for calculating the free energy of a mensicus in the perturbed and unperturbed state.

The stable, critically stable and unstable equilibrium states of a meniscus are all defined in terms of an energy profile, that is, the variation of energy with degree of perturbation. The variational problem of defining parameters for a critically stable meniscus is solved graphically by using a three-dimensional cluster of energy profiles, and it is shown that certain properties of the meniscus, notably volume or pressure, reach limiting values at critical conditions.

Four types of stability are considered for each of three forms of axisymmetric menisci. The stability types are those limited by volume or pressure, in conjunction with limitation by the size of the supporting solid surface or the angle of contact. The three forms of menisci are pendant drops, sessile drops and rod-in-free-surface menisci. Detailed stability criteria are given for each of the twelve different combinations of stability type and meniscus form.

The stability criteria of this study are all derived by numerical interpolation methods applied to the tables of equilibrium meniscus shapes – they are thus theoretical. Where possible they have been compared with experiment and with other studies, and are found to predict critically stable states with an accuracy greater than that likely to be found in the normal course of experiments.

1. Introduction

Tate (1864), a pharmacist, wished to dispense small volumes of liquids from pipettes and syringes. He attempted to show that the amount of liquid falling away from an orifice was constant – in the circumstances this was so. Since then many investigators have attempted to solve the same problem but in every case only empirical equations covering a limited range of data resulted.

The problem of predicting the amount of liquid falling away from an orifice is seen as consisting of three parts:

(i) describing the equilibrium shape of a liquid drop;

(ii) prescribing the particular equilibrium shape of the drop when it reaches critical stability; and

(iii) relating the amount of liquid falling away from the orifice to the critically stable volume and shape and to hydrodynamic factors.

The first part of the problem has been solved for all bounded and unbounded menisci (Bashforth & Adams 1883; Padday 1971; Padday & Pitt 1972*a*; Padday 1972). The shapes of pendant drops as well as of sessile drops, rod-in-free-surface (r.i.f.s.) menisci and liquid bridges have been described in tabular form obtained by a computer integration procedure with Laplace's capillary equation.

The second part of the problem, that of prescribing critical stability conditions, has received much less attention. The most significant contributions in this field are those of Plateau (1873), who solved the gravity-free stability of soap films, and of Lohnstein (1907*a*, *b*, 1913), who investigated the cylindrical and pendant drop meniscus stability in a gravity field.

Though occasionally unrecognized by present workers, Lohnstein obtained the critical stability conditions for one type of pendant drop system, making the intuitive assumption that critical conditions were represented by the maximum drop volume attainable under Laplace equilibrium conditions. He established that as the Bashforth & Adams shape factor β (Bashforth & Adams 1883) was varied, the volume of the drop reached some maximum value. Bouasse (1924), Bakker (1928) and Gillette (1970) review critically and in detail previous studies, including Lohnstein's treatment, and they indicate that no decisive solution to the stability problem of axisymmetric menisci in a gravity field has been found in terms of an energy minimum.

In addition, a large number of experimental studies (Rayleigh 1899; Harkins & Brown 1919; Hayworth & Treybal 1950; Null & Johnson 1958; Poutanen & Johnson 1960; Scheele & Meister 1968; Halligan & Burkhart 1968; Halligan & Agrawal 1971; Izard 1972) have been reported, the best known being that of Harkins & Brown, whose study is currently used for the drop-weight method for surface tension. These studies did not set the criteria for stability. Instead they combined the third or kinetic part of the study with the second part to give useful but nevertheless empirical equations for the breakaway volumes of pendant drops.

In this study we propose an analysis of the second part of the problem only, namely the criteria of critical stability of axisymmetric menisci in a gravity field. The third part, the dynamic factors, does not form a part of this study.

In order to preserve physical reality we have presented the general variational problem as applied to a pendant drop by way of example. However, other types of stability, of pendant drops and of other bounded menisci, will also be considered and the findings of the pendant drop example are applied generally but with great care in the assignation of the signs of the vector quantities.

2. Energy of meniscus formation

Work of forming a meniscus at equilibrium

Consider the energy associated with the growth of a meniscus such as a pendant drop, formed in the manner shown in figure 1. The drop is formed at the tip of a frictionless syringe such that no work is performed on or by the system in transporting liquid from the body of the syringe to the aperture at the tip. The only work done in forming the drop is that due to changes in area of the interfaces and that due to changes in the position of liquid when it passes from the tip to the equilibrium position within a drop.

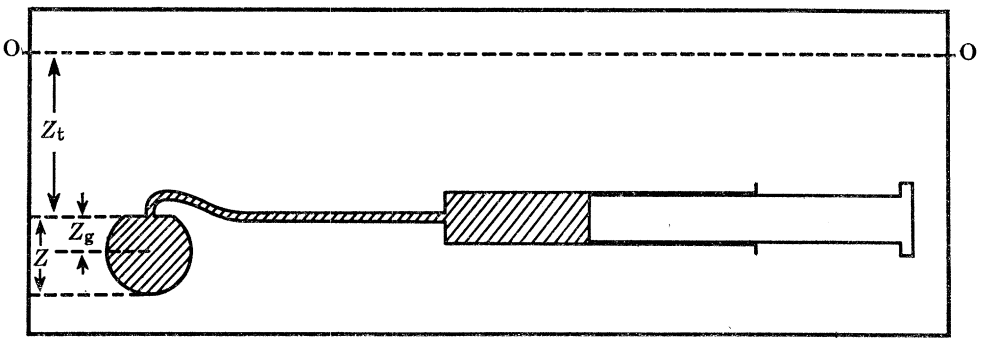

Figure 1. Formation of a pendant drop using a frictionless piston. O–O, level of free surface.

The pendant drop may be successively increased in size by adding small elements of volume, $\mathrm{d}V$ isothermally and reversibly until, at some limiting volume, the drop becomes unstable and a large portion falls away. During this growth the work, W, performed on the system will change and it is this work or energy that we propose to study. The incremental change in the work done, $\mathrm{d}W$, is given by

$$\mathrm{d}W = -p\,\mathrm{d}V_s - V_v\,\mathrm{d}p + \gamma\,\mathrm{d}A - (\gamma_s - \gamma_I)\,\mathrm{d}A' - \mathrm{d}(PE). \tag{1}$$

The first term on the r.h.s. represents the work done when the volume of liquid changes as it passes from the bulk to the miniscus state. Here we consider incompressible liquids only and

dV_s is effectively zero; thus the term will be omitted altogether. The second term accounts for the change in vapour pressure due to the changes in the mean curvature of the liquid–vapour interface as the drop grows. Again for most practical systems this term may be omitted without serious error because the change, $d\phi$, is so very small. The third term on the r.h.s. is the work done in expanding the liquid–vapour interface, the fourth term the work done in changing the area of that portion of the tip in contact with the drop, and the fifth term the potential energy lost by the liquid as the liquid descends from the tip to its equilibrium position in the drop. This last term may be expressed in terms of the volume of the drop and the position of its centre of gravity.

Equation (1) may be modified by substituting for $(\gamma_s - \gamma_I)$ using Young's equation (Young 1804)

$$\gamma_s - \gamma_I = \gamma \cos\theta \tag{2}$$

and for $d(PE)$ according to

$$d(PE) = \rho g V \, dZg + \rho g Zg \, dV \tag{3}$$

so as to give

$$dW = \gamma dA - 2\pi X \, dX \gamma \cos\theta - \rho g V \, dZg - \rho g Zg \, dV, \tag{4}$$

where the change in tip area is given by

$$dA' = 2\pi X \, dX. \tag{5}$$

As the pressure on the syringe plunger equals the pressure within the liquid at the tip, the incremental work, dW, is given by,

$$dW = \rho g Z_t dV, \tag{6}$$

where $\rho g Z_t$, the hydrostatic pressure at the tip, is a characteristic property of the meniscus. Equations (4) and (6) may now be combined and made dimensionless by dividing by appropriate powers of k, the meniscus coefficient, where

$$k = (\gamma/\rho g)^{\frac{1}{2}} \tag{7}$$

to give

$$dW/\gamma k^2 = Z_t dV/k^4 = dA/k^2 - 2\pi X \, dX \cos\theta/k^2 - (Zg \, dV + V \, dZg)/k^4. \tag{8}$$

The integral form of equation (8) is thus:

$$W/\gamma k^2 = \int_{V=0}^{V=V} Z_t dV/k^4 = (A - A_0)/k^2 - (X^2 - X_0^2)\, \pi \cos\theta/k^2 - VZg/k^4. \tag{9}$$

These equations apply only to a single component liquid in contact with vapour and with an insoluble tip, and it is assumed that ρ and g are constant throughout the system.

Work of forming a meniscus not at equilibrium

The pendant drop formed by the process of equilibrium growth can possess only one stable shape and then only when its volume is less than the volume of the critically stable drop. However, it is clear that a given volume may possess an infinite variety of shapes each of which possesses a different work of formation.

The work done on the system to create a drop of any arbitrary shape will still be given by equations (4), (8) and (9). Such a drop can only exist transiently and is called perturbed to distinguish it from the drop which rests at equilibrium.

Everett & Haynes (1972) indicate that at constant temperature and constant volume of vapour in the system, W may be identified with the Helmholtz free energy of the meniscus in

excess of that which the liquid would have in the bulk state. The identification of the change in Helmholtz free energy, dF, with dW is given in Appendix A. It can also be obtained from Buff's treatment of the thermodynamics of curved surfaces (Buff 1960).

Comparison with Buff shows clearly we have assumed that:

(i) The curvature of the surface does not affect the value of surface tension. For small radii of curvature ($< 10^{-8}$ m) the assumption can lead to significant errors, but such radii are outside the scope of this study.

(ii) The volume of the liquid does not change measurably when passing from bulk to surface state. This assumption restricts our analysis to conditions well removed from the critical temperature.

(iii) The liquid forming the drop is pure and in contact with its vapour and an insoluble solid only.

It is, of course, possible to include for these other effects using Buff's extra terms in equations (8) and (9).

The energy profile of a meniscus

The energy profile of a meniscus is defined as the integral work or free energy of a drop, according to equation (9), expressed as a function of the degree of perturbation. The perturbations that may be imposed on an equilibrium drop can follow an infinite number of paths, but in this study we consider axisymmetric perturbations from one 'Laplace shape' to another. A 'Laplace shape' is defined here as an axisymmetric drop shape wherein the sum of the principal curvatures varies linearly with vertical distance from a fixed point.

In physical terms this type of axisymmetric perturbation would occur if the gravitational acceleration were momentarily altered to change the drop to some new equilibrium shape and then returned instantly to its initial value. The perturbed drop would then be in a non-equilibrium shape and its energy is calculated according to equation (9) but with the unperturbed value of g or k. The perturbation is equivalent to 'flicking' a pendant drop on a rod, which if done with sufficient force, will dislodge it.

In this study we make the hypothesis that perturbations of a meniscus from one axisymmetric 'Laplace shape' to another are perturbations of lowest energy and thus are those which are most likely to occur and to yield the critical properties.

By restricting the perturbations of this study to those that conform to a 'Laplace shape', the degree of perturbation may now be assessed quantitatively from a shape factor such as that defined by Bashforth & Adams (1883). They showed that the shape of a pendant (or sessile) drop could be given in terms of characteristic parameters of the system according to

$$\beta = \rho g b^2/\gamma = b^2/k^2, \tag{10}$$

where β was the shape factor. This shape factor is very suitable for expressing the perturbation of a drop quantitatively. Other properties such as meniscus angle, ϕ, the height, Z, of the drop and the position of the centre of gravity, Zg, in relation to the tip are all dependent on β and hence are equally useful in expressing the degree of perturbation numerically.

The energy profile of a pendant drop as a function of the perturbation, β, is shown in figure 2. In addition the shape profiles at selected points on the curve are shown at the top of the diagram. The energy profile is not defined by the equilibrium shape alone. One must further define the conditions under which perturbation takes place. In the example of the pendant drop of figure 1 these conditions of perturbation are given as radius limited and volume limited. This means

that during the process of perturbation the radius of contact of the drop with the tip and the volume of the drop both remain fixed.

The method for calculating the energy of a meniscus in its perturbed or unperturbed state using tables of shape properties is given in appendix B. The tables (Padday 1972) used for deriving energy profiles were obtained by integrating the capillary equation of Young (1804) and Laplace (1805),

$$\gamma(1/R_h + 1/R_v) = \rho g Z_t, \tag{11}$$

which in dimensionless form is

$$k/R_h + k/R_v = Z_t/k. \tag{12}$$

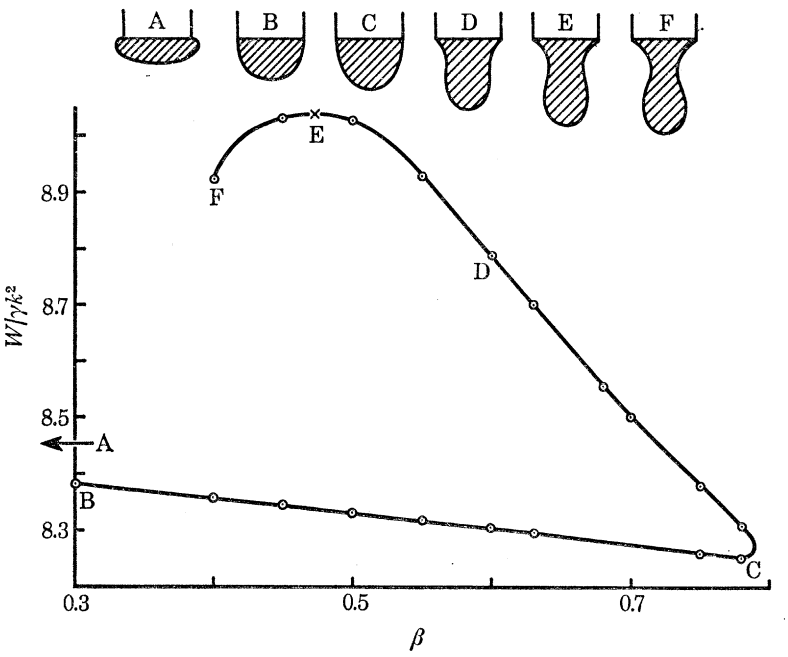

FIGURE 2. Energy profile of a pendant drop. Work of formation as a function of perturbation. $X/k = 1.200$; $V/k^3 = 4.9638$; C is position of stable equilibrium and E is position of unstable equilibrium. Shape profiles are given for the points indicated except for A which is off the graph.

The tables contain the coordinates of the shape, the principal radii of curvature, the integrated areas and volumes, and in some the integrated moment (PE) of the volume about the free liquid level. Thus with these tables one has all the data required to derive the energy profile.

The method by which each energy point is found is essentially a location or interpolative procedure. The value of V/X^3 is known from starting or experimental conditions, and all that is necessary is to find the position within a given profile at which V/X^3 equals the fixed value. At this position the shape and boundary conditions are now fixed, but not the size. The profile shape is then scaled to the correct tip size by multiplying with an appropriate magnification factor, M, such that the value of X/k obtained from the tables equals the experimental value. The integral meniscus energy is then obtained by subtracting the potential energy term from the area terms. Other points at different shapes or β values are now sought and evaluated in the same way until the whole energy profile, such as that of figure 2, is established.

For a given shape, β, there are two points at which V/X^3 (experimental) equals the ratio obtained in the tables. This arises because within a given shape profile the value of V/X^3 increases from zero to some maximum value and then decreases, provided V/X^3 experimental

is less than the maximum value of the profile. It must be emphasized that the maximum value of β, which is seen in figure 2, does not correspond to the position of minimum energy.

The energy profile of figure 2 possesses two equilibrium positions where

$$(\mathrm{d}W/\mathrm{d}\beta)_{T,V,X,k} = 0. \tag{13}$$

At the lower position, C, where W obtains a minimum value, the drop is in stable equilibrium and at the upper position, E, the drop is in unstable equilibrium. At each of these points, but not at any other position, the drop is in true 'Young–Laplace' equilibrium and the magnification factor, M, becomes equal to unity.

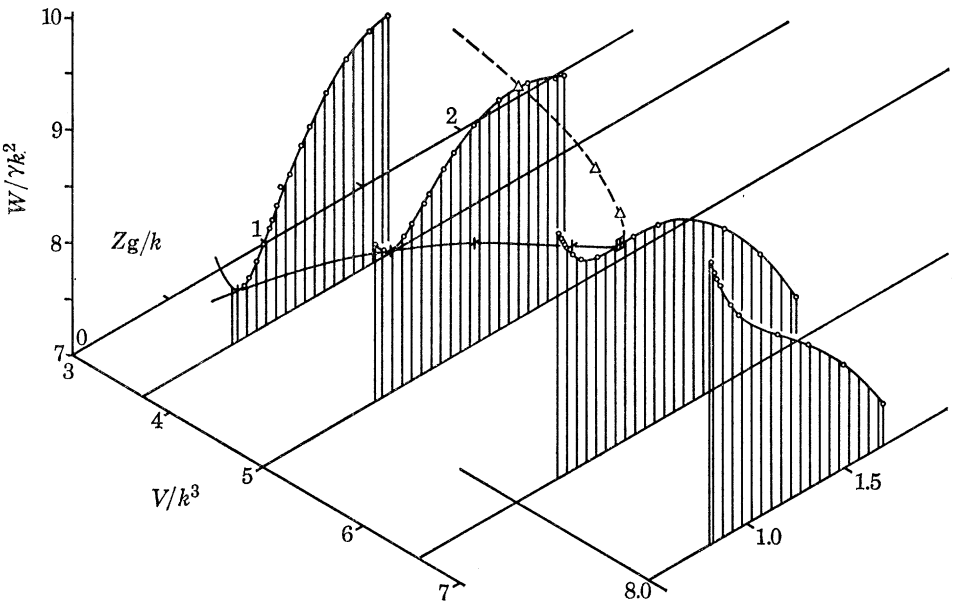

FIGURE 3. Energy profiles as a function of pendant drop volume. +, points at stable equilibrium; △, points at unstable equilibrium; ⊞, point at critical equilibrium; ○, points unstable and not at equilibrium.

The energy profile of figure 2 is that of a drop which can exist at stable equilibrium. As the volume of the drop is increased, so the energy profile changes in shape as is seen in figure 3. In this figure the energy profile of figure 2 is plotted with Zg/k instead of β as the measure of the degree of perturbation. This is done in order to emphasize the maxima and minima that occur in the energy profiles of those drops of small volume. Four energy profiles, each of different but constant volume, are shown and all refer to a single tip radius. The two profiles for small volume show the maxima and minima of the unstable and stable equilibrium states referred to in table 1. As the volume of the drop increases so the unstable and stable equilibrium points come closer together until at the critical volume the two points merge and the profile no longer possesses a minimum but only an inflexion point. At this critical meniscus volume

$$(\mathrm{d}^2W/\mathrm{d}\beta^2)_{T,V,X,k} = (\mathrm{d}^2W/\mathrm{d}Z_{\mathrm{g}}^2)_{T,V,X,k} = 0. \tag{14}$$

This critical meniscus point is the position being sought in this study. Once found, it enables all critical meniscus properties to be obtained.

Energetically, a meniscus may be in any of four states: stable equilibrium, unstable equilibrium, critical equilibrium and non-equilibrium. The definitive energy criteria of these four states are given in table 1. Only the stable equilibrium may be obtained experimentally; all other shapes are obtained transiently only.

TABLE 1. CRITERIA FOR EQUILIBRIUM AND STABILITY OF AXISYMMETRIC MENISCI

state	$dW/d\beta$ or $dW/d\phi$	$d^2W/d\beta^2$ or $d^2W/d\phi^2$
stable equilibrium	$= 0$	> 0
unstable equilibrium	$= 0$	< 0
critical equilibrium	$= 0$	$= 0$
non-equilibrium (unstable)	$\neq 0$	—

The variational problem

The construction of energy profiles in order to obtain the properties of a meniscus in its critical equilibrium state is tedious and time-consuming. Instead, we have found a solution to the variational problem which has allowed the critical conditions of a meniscus to be sought in terms of the first order variation of an easily measured property.

The work of formation of free energy of an axisymmetric meniscus, as defined by equation (9), may be shown to be a function of three independent variables of which

$$W/\gamma k^2 = f_1(\beta, V/k^3, X/k) \tag{15}$$

is an obvious example; V/k^3, X/k and β define the size and shape of the meniscus and its degree of perturbation.

At equilibrium, the first differential, equation (8), must be zero; hence a degree of freedom, in this case β, is lost. Under conditions of critical equilibrium the second differential also equals zero, and a further degree of freedom, in this case the volume V/k^3, is lost. Thus at critical equilibrium the state being sought in this study, the tip size X/k completely specifies the system and the critical meniscus volume, together with other critical properties, is dependent on X/k alone.

The work of formation in an equilibrium state is given by

$$W/\gamma k^2 = f_2(V/k^3, X/k) \tag{16}$$

and that in a critical state is given by

$$W/\gamma k^2 = f_3(X/k). \tag{17}$$

Equation (16) is a function such that for a fixed value of V/k^3 and X/k two solutions are possible.

As V/k^3 is increased at constant tip size these two equilibrium values of the energy converge until at critical equilibrium the two values reach a single maximum value. At this point we find that no further equilibrium values of V/k^3 may be found in excess of the critical volume and therefore this value attains a maximum and

$$(dV/k^3 d\beta)_{T,X,k} = 0. \tag{18}$$

That a pendant drop must reach this maximum volume at critical conditions was first suggested by Lohnstein (1907*a*) (cf. Bakker 1928).

The occurrence of a maximum volume at critical equilibrium may be shown algebraically by considering the sign and magnitude of each term in equation (9), in its first-order differential, equation (8), and in its second-order differential. However, a much clearer explanation is given by plotting out a series of energy profiles in a three-dimensional graph as in figure 3.

In this figure the energy of a pendant drop of fixed tip-radius X/k is plotted as a function of both volume V/k^3 and the perturbation. We have already noted that the degree of perturbation

may be estimated from other characteristics of the meniscus and here we have used the depth of the centre of gravity of the drop below the tip; by using this criterion the energy profile is extended and prevented from looping over on itself and thereby obscuring the maxima and minima.

Four energy profiles are shown in figure 3. The first two profiles at the smaller volumes are those with clearly visible stable and unstable equilibrium states. The third energy profile is that of the critical meniscus state, and the fourth energy profile is that of a drop, the volume of which is larger than the volume of the critical state and therefore is never at equilibrium. Clearly this fourth state cannot be obtained experimentally.

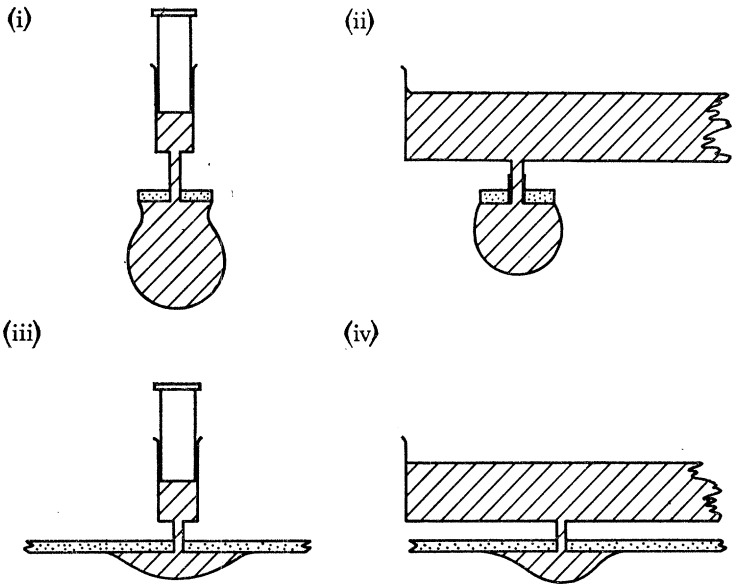

FIGURE 4. Types of pendant drop stability: (i) volume–radius limited; (ii) pressure–radius limited; (iii) volume–angle limited; (iv) pressure–angle limited.

The energy surface of figure 3 is a plot of f_1 (β, V/k^3, X/k) with the value X/k fixed and β expressed as Zg/k. The continuous line between the energy profiles connects the stable equilibrium points, and the broken line the unstable equilibrium points. These two lines meet at the condition of critical stability and show quite clearly that $\mathrm{d}V/\mathrm{d}Zg$, and hence $\mathrm{d}V/\mathrm{d}\beta$, equal zero. *Thus at critical equilibrium the volume of liquid forming this particular drop reaches a maximum value.*

So far, the treatment has been applied to only one type of stability of one form of bounded meniscus. In the more general treatment we propose to show that the same procedure may be applied to evaluate the critical stability criteria of many other types of axisymmetric menisci.

Stability of different forms of menisci

We have investigated differing types of stability associated with the three different types of bounded menisci (Padday 1971); sessile drops, pendant drops and rod-in-free-surface (r.i.f.s.). Four different types of stability may be devised experimentally for pendant drops and these are shown in figure 4. In this figure, the first type, described here as that with volume-radius limited stability, is the example already considered. The other types of stability and their criteria are given in table 2.

In forming a pendant drop by successively increasing its volume, the pressure inside the

liquid at the plane of the tip first increases and then, after reaching some maximum value, decreases. In order to demonstrate this effect, the pressures at two tips of different sizes have been plotted diagrammatically with increasing volume in figure 5. In this figure, 15 separate shapes of different β values have been drawn to scale and have been placed at a distance from the free liquid level such that the vertical scale represents the hydrostatic pressure at all points on each meniscus. Each meniscus is now cut off in a plane corresponding to $X/k = 0.2$, and the position of this plane on the vertical axis represents the pressure at the tip. The shapes of larger β values are also cut in planes corresponding to the larger tip, $X/k = 1.2$. It is thus seen that the pressure at both tips first increases, then decreases before reaching the value limited by volume.

TABLE 2. TYPES OF MENISCUS STABILITY AND THEIR CRITICAL EQUILIBRIUM CONDITION

(i) volume–radius limited	$(\mathrm{d}(V/k^3)/\mathrm{d}\beta)_{T,k,X} = 0$
(ii) pressure–radius limited	$(\mathrm{d}(Zt/k)/\mathrm{d}\beta)_{T,k,X} = 0$
(iii) volume–angle limited	$(\mathrm{d}(V/k^3)/\mathrm{d}\beta)_{T,k,\phi} = 0$
(iv) pressure–angle limited	$(\mathrm{d}(Zt/k)/\mathrm{d}\beta)_{T,k,\phi} = 0$

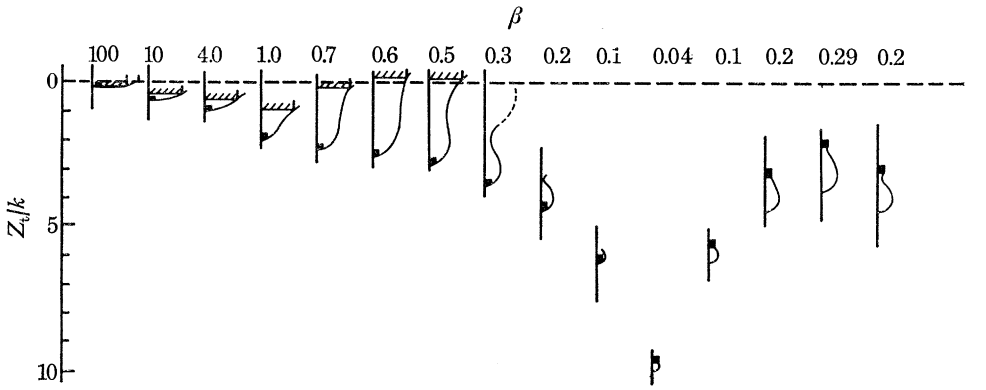

FIGURE 5. Growth of pendant drops: each profile is drawn to scale and is positioned in its correct relative position to the free surface. ▨, position of tip $X/k = 1.2$; ▬, position of tip $X/k = 0.2$. β values are indicated.

The shape factor corresponding to the maximum tip pressure gives the critical condition for the stability of a pendant drop formed with a constant pressure head as shown in figures 4(ii). This system is designated the pressure–radius limited system. Perturbations of the pressure-radius limited pendant drop will now involve a change in volume of the drop. Below the maximum pressure, small volume changes will always be balanced by pressure changes which prevent further diminution or growth. However, when the maximum pressure is reached, any increase in volume now results in uncontrolled growth until detachment takes place.

Energy diagrams of the type given in figure 3 show clearly that the critical energy condition of table 1 corresponds to this maximum pressure where

$$(\mathrm{d}Z_t/k\,\mathrm{d}\beta)_{T,X,k} = 0. \tag{19}$$

It must be emphasized that the change in direction of β that occurs in the region of this critical condition again does not correspond exactly with the critical condition, and serious errors can arise if such an assumption is made. Also, the centre of gravity Zg is not at its maximum distance from the free surface at the point of critical pressure.

Further types of stability are found when the liquid forming the drop forms a finite angle of contact with the solid supporting the drop. With such systems the meniscus angle, ϕ, can never

be less than the contact angle, θ, except when the drop is supported by the liquid in the orifice of the tip. Thus when, during the growth of the drop, ϕ reaches the value of θ, the drop spreads along the under surface of the tip and X/k is no longer constant. Systems such as those shown in figures 4 (iii) and (iv) are designated volume–angle and pressure–angle limited pendant drops respectively.

Equation (9) is basically, the fundamental equation from which the energies of all four types of menisci were derived. However, some of the terms in the equation remain constant either during growth or during perturbation, hence the equation may be simplified to the following working equations for use within the limitations given:

(i) for all radius limited menisci,

$$(W/\gamma k^2)_{T,X,k} = A/k^2 - ZgV/k^4 + C, \tag{20}$$

where

$$C = A_0/k^2 = \pi X^2/k^2 \tag{21}$$

and

$$(\mathrm{d}W/\gamma k^2)_{T,X,k} = \mathrm{d}A/k^2 - \mathrm{d}(VZg)/k^4, \tag{22}$$

which for volume–radius limited perturbations becomes

$$(\mathrm{d}W/\gamma k^2)_{T,X,V,k} = \mathrm{d}A/k^2 - V\,\mathrm{d}Zg/k^4; \tag{23}$$

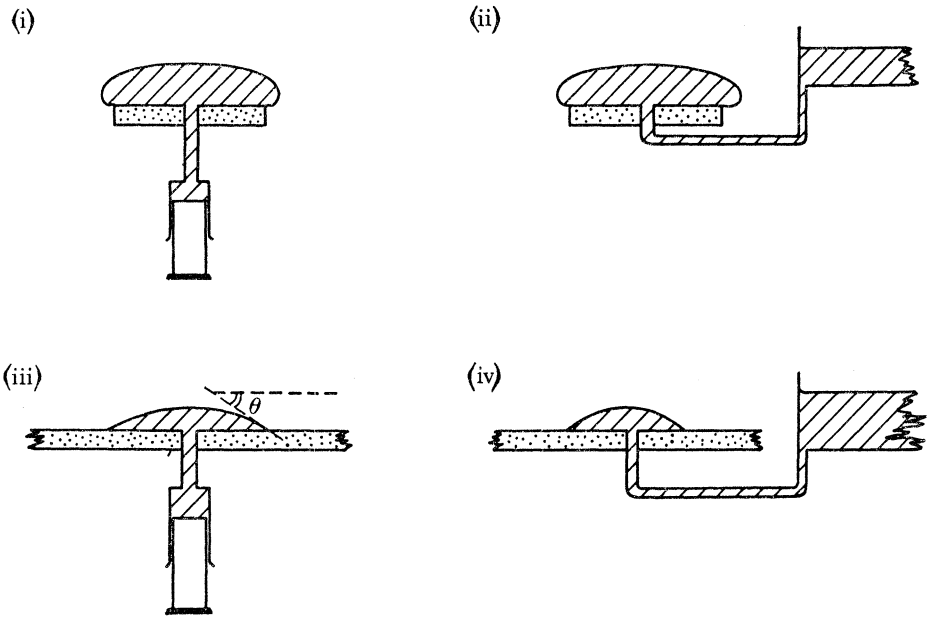

FIGURE 6. Types of sessile drop stability: (i) volume–radius limited; (ii) pressure–radius limited, (iii) volume–angle limited; (iv) pressure–angle limited.

(ii) and for all angle limited menisci

$$(W/\gamma k^2)_{T,\phi,k} = A/k^2 - \pi X^2 \cos\theta/k^2 - VZg/k^4 + C, \tag{24}$$

where

$$C = \pi X_0^2(\cos\theta - 1) \tag{25}$$

and

$$(\mathrm{d}W/\gamma k^2)_{T,\phi,k} = \mathrm{d}A/k^2 - 2\pi X\,\mathrm{d}X\cos\theta/k^2 - \mathrm{d}(VZg)/k^4, \tag{26}$$

which for volume–angle limited perturbations becomes

$$(\mathrm{d}W/\gamma k^2)_{T,V,\phi,k} = \mathrm{d}A/k^2 - 2\pi X\,\mathrm{d}X\cos\theta/k^2 - V\,\mathrm{d}Zg/k^4. \tag{27}$$

Many energy profiles have been constructed with these equations, and in every case we find that the conditions we have adopted for critical stability given in table 2 are found precisely at values corresponding to the criteria given in table 1.

The pendant drop meniscus is only one of the three types of bounded meniscus, and here we have extended the study to include stability conditions of sessile drops and r.i.f.s. menisci. Diagrammatic representations of these latter systems are shown in figure 6 for sessile drops and figure 7 for r.i.f.s. menisci.

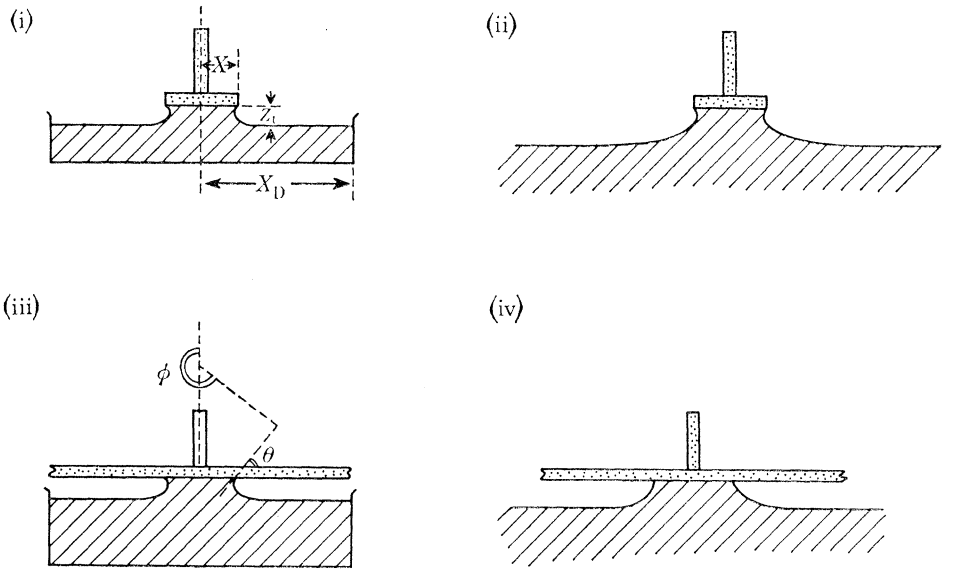

FIGURE 7. Types of rod-in-free-surface stability: (i) volume–radius limited; (ii) pressure–radius limited; (iii) volume–angle limited; (iv) pressure–angle limited.

We have found that the energy profiles calculated according to equations (20) to (27) apply equally well to sessile drops and r.i.f.s. menisci, with the exception that the area and potential energy terms of the r.i.f.s. menisci are now summed instead of subtracted. In this way we have established the properties of the menisci at critical stability for the four different types of limitation of the three meniscus forms, pendant drops, sessile drops and r.i.f.s. systems.

3. Methods for extracting critical properties from profile tables

The maximum or critical volume that may be supported by a tip of known size in the volume–radius limited pendant drop may be obtained in principle by constructing sufficient energy profiles in figure 3.

A second method involves extracting the value of V/k^3 at constant X/k from the tables (Padday 1972) and then plotting V/k^3 as a function of the shape factor β of each table. Such a plot reveals the maximum value provided the set of tables possess sufficiently small increments in β. For most systems this is usually so, and the final results may be obtained very accurately when a satisfactory interpolation procedure is used. Though much simpler than the energy profile method, this interpolation procedure is still lengthy.

A third method, the one used widely in this study, is by far the simplest and is sufficiently accurate for all experimental purposes. This method is called 'the envelope construction method', and involves plotting a series of functions and then drawing the function that envelopes all the other functions.

When we evaluate the properties of the volume–radius limited pendant drop, the value V/k^3 is plotted as a continuous function of X/k for a given shape, β. This same operation is then repeated for other fixed values of β until the whole graph is built up as a network of shapes as in figure 8. The graph possesses a clearly defined border or envelope, and this border gives the critical volume as a function of X/k. In figure 8, only parts of the individual functions are plotted, for clarity.

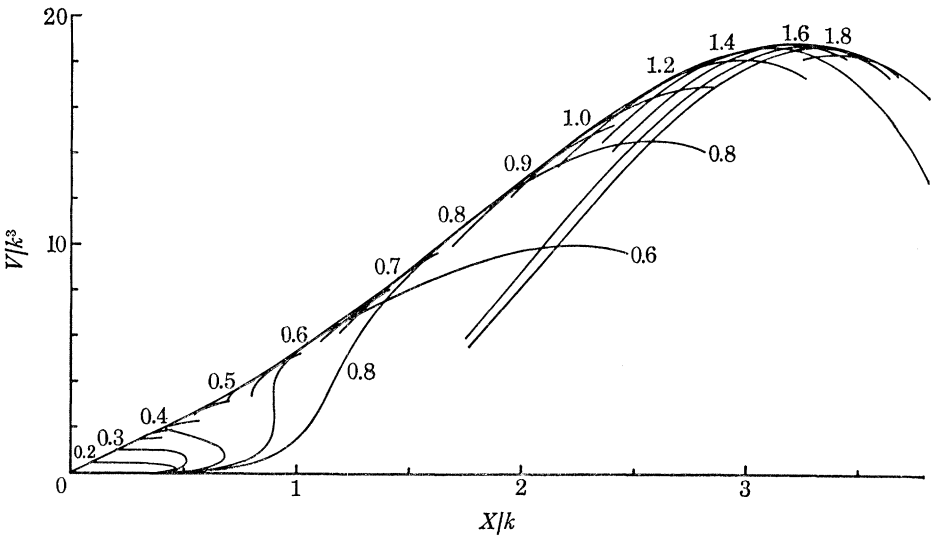

FIGURE 8. Volume of a pendant drop as a function of tip radius. Shape factors β are shown for some of the profiles: the envelope curve is the critical volume as a function of tip radius.

These plots were obtained with a Hewlett-Packard 9100A calculator coupled to a 9125A automatic plotter. Precision graph paper was used and a plotting accuracy of ± 0.005 cm was obtained. Computer programs, already described (Padday 1971, 1972), were written in simple machine code which performed a step-by-step integration of the local equilibrium of the Laplace equation. The envelope line was constructed with the use of a flexible curve. This method would not have been practicable without the automatic plotter.

Other properties such as pressure, angle of contact, meniscus height and shape factor for the critically stable condition were obtained from interpolation in the tables using the critical value of V/k^3 and X/k obtained from the envelope construction graph.

4. STABILITY OF PENDANT DROPS

The growth and the general conditions that lead to the instability of a pendant drop have already been outlined in the introduction. It is also noted that the four different pendant drop systems shown in figure 4 are those for which we give the conditions of critically stable equilibrium. These data apply equally to an emergent bubble.

Volume–radius limited pendant drop

This type of drop is formed according to the system of figure 4(i). The tip is assumed to be fully wetted; hence X/k remains constant as the volume of the drop is increased successively from zero, in the manner already described in reference to figure 5.

At the birth of the drop the meniscus angle ϕ is zero and $\beta = \infty$ (for a flat surface). As the drop grows ϕ increases and β decreases. Though Bashforth & Adams (1883) and Padday (1971) designate β as being negative for pendant drops, we have not used this convention here but rather have retained β as being always positive. This is so that the square root of β in equation (7) possesses real values only.

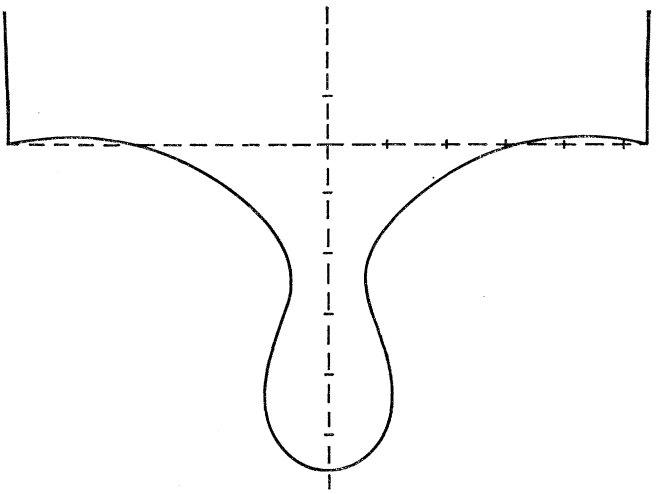

FIGURE 9. Shape of critical pendant drop when X/k is very large. (> 3.2) 'Bath tap profile'. $\phi < 0°$. $X/k = 5.4$.

During the initial stage of growth the hydrostatic pressure in the liquid at the tip increases with volume. If the meniscus angle reaches 90° (i.e. only when the tip is relatively small) the shape factor attains a minimum value and further increases in volume result in β increasing. In the vicinity of, but not at, $\phi = 90°$ the tip-pressure reaches a maximum value. Further growth in volume continues until the inflexion point in the profile is reached when the meniscus angle obtains a maximum value. If the radius of the tip is relatively large, then the inflexion point is reached before $\phi = 90°$, and in this event, the shape factor does not change direction during growth of the drop. From this inflexion point, as for all tips, the drop continues to grow with ϕ now decreasing, until finally the critical volume is reached. All these growth patterns are best understood by studying figure 5 carefully and comparing the shapes with a set of tables.

An important feature of the condition for critical stability of the volume–radius limited pendant drop is that the position of the tip lies between the first and second inflexion points on the drop profile.

The maximum or critical volume was obtained by the envelope construction method already given in figure 8. This figure not only shows clearly that a maximum volume is reached but also that the volume curve of each shape factor crosses all other curves once only. This means that at each intersection two Laplace solutions exist. Inspection now reveals that one curve represents stable equilibrium (at a point on the curve between the origin and the critical point) while the

other curve represents an unstable equilibrium (at a point on the curve which has passed the critical point). These two Laplace solutions are the points C and E on the energy profile in figure 2.

The profile of a pendant drop formed at small tips is part of a profile consisting of a multiplicity of distorted unduloids (Padday 1971). For these menisci, multiple solutions appear to give rise to a series of unstable equilibrium states. However, these states have little practical significance because they cannot be approached from a stable state.

An important feature emerging from figure 8 is that the critical volume itself reaches a maximum value (when $X/k \approx 3.2$). At this point the meniscus angle reaches a value $\phi = 0°$. However, stability criteria do not cease to apply at this point and at even larger values of X/k the stability now refers to the meniscus formed at an orifice, such as that of figure 9. This is the form of a drop as it breaks away from a large orifice such as that of a bath tap.

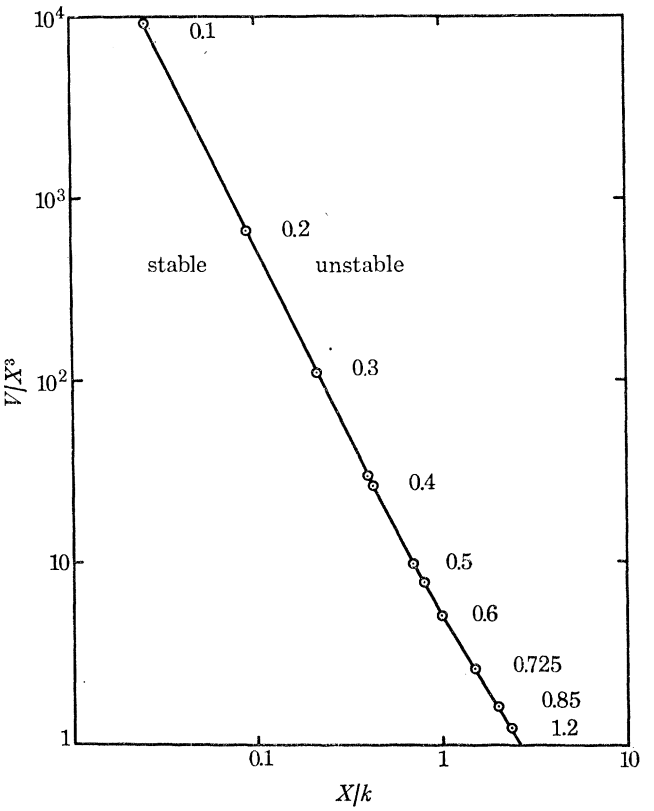

FIGURE 10. Pendant-drop stability: critical volume ratio of a volume–radius limited drop as a function of tip radius. β values are indicated.

Experimentally one measures both V and X, k often is unknown. A more useful form of the critical volume data of the volume–radius limited pendant drop is given in figure 10, in which V/X^3 corresponds to the volume ratio of the critical shape. The volume falling away is always less than the critical volume, firstly because experimental vibration promotes instability at an earlier stage of drop formation, and secondly because the whole volume does not fall away.

The meniscus angle, ϕ for conditions of critical stability, varies with tip radius as shown in figure 11. This figure indicates that for small tip radii the angle $\phi \simeq 90°$ and the liquid is held just above the narrowest point of the neck of the profile. As the tips become larger, so the angle

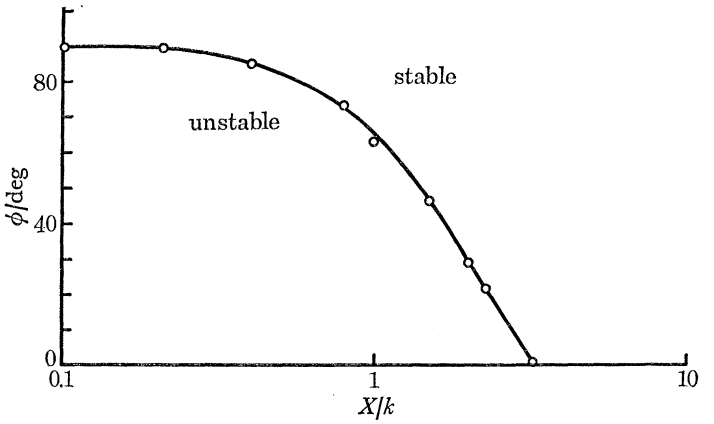

FIGURE 11. Pendant-drop stability: critical meniscus angle of volume–radius limited drop as a function of tip radius.

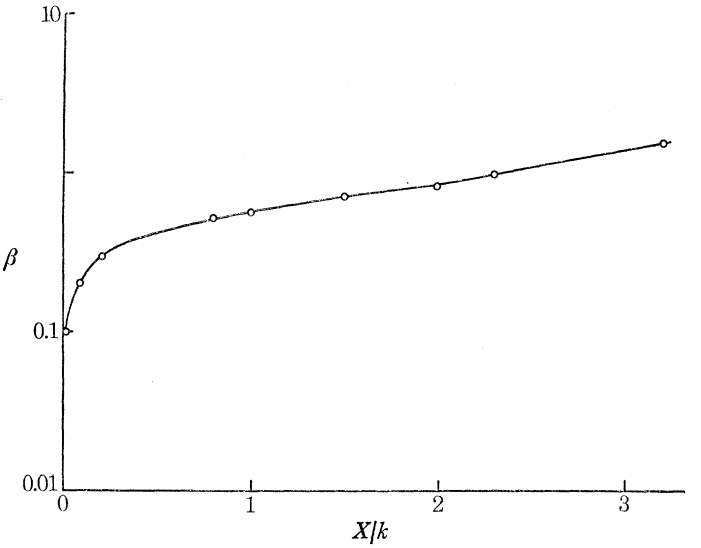

FIGURE 12. Pendant–drop stability: critical shape factor of a volume–radius limited drop as a function of tip radius.

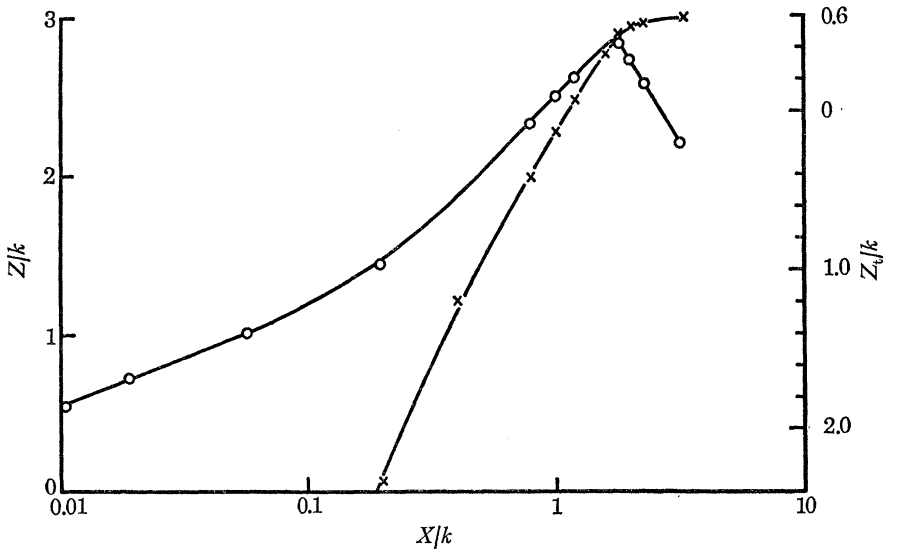

FIGURE 13. Pendant-drop stability: critical height, Z/k (O) and critical pressure, Z_t/k (×), of a volume-radius limited drop as a function of tip radius.

PHILOSOPHICAL TRANSACTIONS OF THE ROYAL SOCIETY A MATHEMATICAL, PHYSICAL & ENGINEERING SCIENCES

at which critical conditions are reached decreases to zero. Further increase in tip size results in the shape of the critically stable profile taking the 'bath tap' configuration of figure 9. In this situation the angle becomes negative.

In figure 12 the shape factor β of the critically stable pendant drop is plotted as a function of tip radius. This plot enables the critical shape of the drop to be sought in the tables. An interesting feature of this plot is that almost all shapes of practical interest lie in the region $\beta = 0.1$ to 1.0.

The tip pressure of a volume–radius limited drop at critical equilibrium is very much less than the maximum pressure shown in figure 5. We have therefore plotted this tip pressure Z_t/k for conditions of critical stability in figure 13. An important feature of this curve is that for large tip radii, $X/k > 1.1$, the tip pressure assumes a negative value; the tip being above the level of the free flat surface. Figure 13 also shows the actual height, Z/k, of the pendant drop in its critical state. The height of the drop increases, as expected, with tip radius, but when X/k reaches approximately 1.7, the height passes through a maximum value and then decreases. Large drops are thus much flatter in shape.

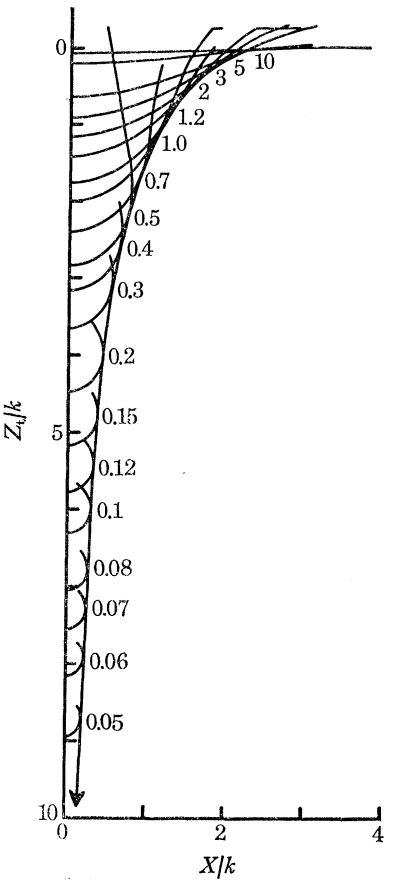

FIGURE 14. Pendant-drop stability: pressure of a drop as a function of tip radius: the envelope curve is the critical pressure as a function of the tip radius. Shape factors β are shown for some profiles.

Pressure–radius limited pendant drop

A pendant drop system of this type is shown in figure 4 (ii), and its growth, caused by successively increasing the hydrostatic pressure, has already been described. The critical conditions

for this system are given in table 2 and are obtained when the pressure at the tip supporting the drop reaches a maximum value. The growth to this point is shown diagrammatically in figure 5.

We obtained the maximum pressure at the tip supporting the drop by the envelope construction method and also by direct interpolation from the tables: both methods agreed very well. The plot of figure 14 shows the shapes of pendant drops of successive β values plotted in such a way that every point on each profile corresponds to its correct hydrostatic height. The envelope curve of this figure thus becomes the maximum pressure curve and represents the stability criteria being sought. The stability criteria at tips of small radii are very difficult to interpolate and so critical pressures in this region are plotted separately in figure 15, again as a function of X/k, but with the ordinate on a logarithmic scale.

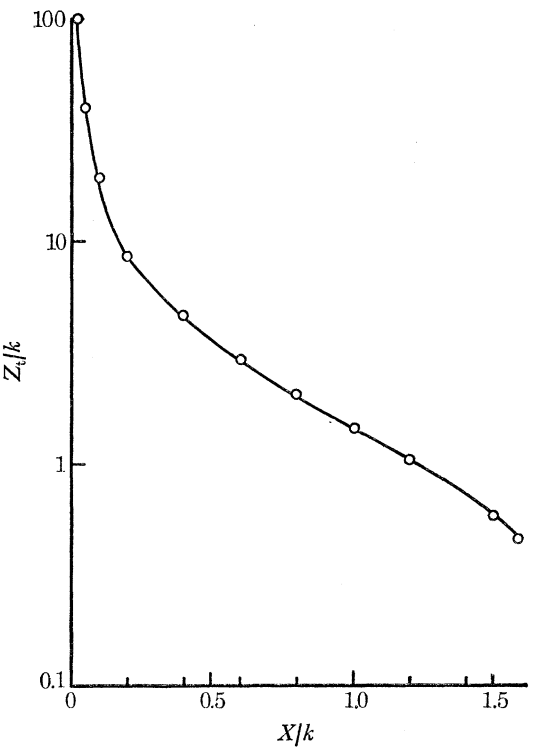

FIGURE 15. Pendant-drop stability: critical pressure of a pressure–radius limited drop as a function of tip radius.

The critical pressure at small tips, $X/k < 0.5$, occurs when the meniscus angle is very nearly 90° and the pendant drop approximates to a hemisphere. For these conditions

$$\rho g Z_t = 2\gamma \sin\phi/X \approx (2\gamma/X)_{\phi=90°} \tag{28}$$

or

$$Z_t/k = 2k/X. \tag{29}$$

The main use of the stability data of pressure–radius limited pendant drops lies in predicting the head of liquid required to start flow through a jet, the tip of which is fully wetted. Again, we emphasize that these critical pressures do not correspond to the shapes where the centre of gravity Zg is at a maximum.

Volume–angle limited pendant drop

A pendant drop may be formed at a very large tip rather as that shown in figure 4(iii). In this example the pendant drop builds up in a series of stable equilibrium states by the addition of liquid through an orifice in the plate or tip. At first the tip is unwetted and only the orifice supports the meniscus. When the meniscus angle ϕ reaches the value of the contact angle θ, the drop spreads out along the plate at constant angle $\phi = \theta$ until critical conditions initiate break away. At critical conditions the volume of the drop reaches a maximum equilibrium value.

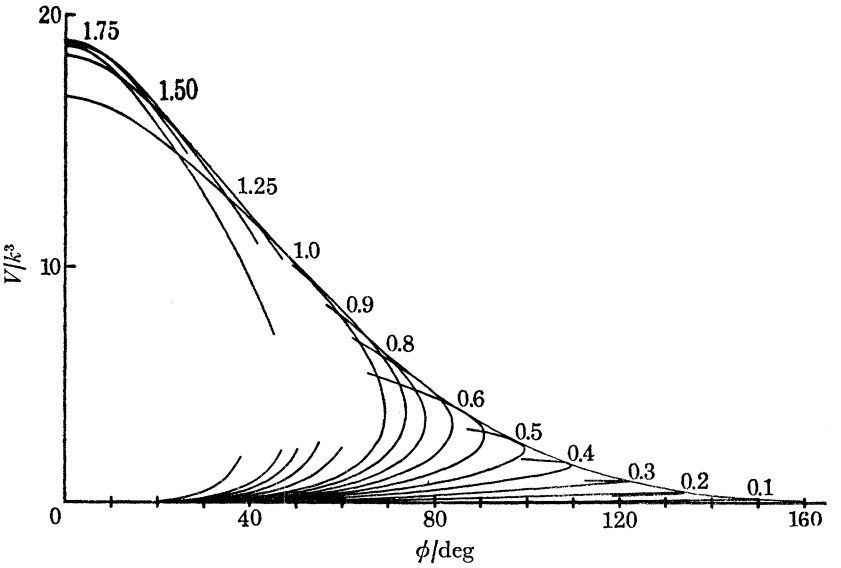

FIGURE 16. Pendant-drop stability: volume of a volume–angle limited drop as a function of meniscus angle. The envelope curve is the critical volume as a function of the meniscus angle where $\phi = \theta$. Shape factors β are shown for some profiles.

In figure 16 we have plotted the volume V/k^3 as a function of meniscus angle for profiles of 16 different β values and have constructed the envelope function to give the volume at critical stability as a function of angle.

The most interesting feature to emerge from this figure is that at $\phi = 0°$ the critical volume reaches a well-defined maximum value which corresponds to the maximum of figure 8. This maximum volume is that of a critically stable drop hanging from a fully wetted ceiling. As already noted, the angle of the critical meniscus of figure 16 may become negative for the system of figure 9, but these values have not been included in the graph.

These data give the complete stability criteria for the pendant drop detachment from the outside of a cone, the system investigated by Brown & McCormick, (1948).

Pressure–angle limited pendant drop

This system consists of a large plate with a small orifice in it connected to a constant pressure head, the hydrostatic height of which can be successively increased. The meniscus one might expect to form is shown in figure 4(iv).

Experimentally a meniscus forms on the underside of the plate at the orifice and the drop then grows in size with the meniscus angle increasing until it equals that of the contact angle of

the liquid on the solid. Growth up to this point is volume–radius limited, the radius being that of the orifice, and as growth continues, the pressure increases. Provided that the orifice is relatively small, the maximum pressure at the tip is reached when the meniscus angle equals the contact angle.

Any further increase in volume now results in spreading on the underside of the plate. As spreading takes place X/k increases resulting in a decrease in tip pressure (figure 13) and hence unstable growth. When the contact angle condition is met and the maximum pressure is reached, further uncontrolled growth takes place as though the pendant drop were volume–angle limited. When maximum volume is reached the drop falls away.

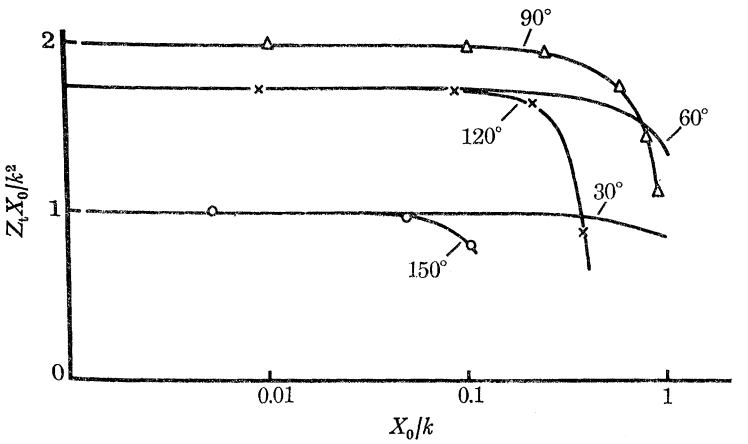

FIGURE 17. Pendant-drop stability: critical pressure product ($Z_t X_0/k^2$) of a pressure–angle limited meniscus as a function of orifice radius. Contact angles are indicated.

In figure 17 the product of the critical orifice pressure Z_t/k and the orifice radius X_0/k is plotted as a function of the orifice radius for five different angles of contact. When the orifice radius is small, $X_0/k < 0.05$, it is clear that the tip pressure is given by the relation of equation (28) but with X substituted by X_0. For larger orifices the pressure at critical conditions decreases, until for very large orifices the contact angle condition is never met and the stability criterion is volume–radius limited. For poorly wetted surfaces, when $\theta > 90°$ the angle criterion may never be met because as already noted, the meniscus angle itself reaches a maximum value (at the inflexion point on the profile). Thus, if the maximum meniscus angle is always less than the contact angle the pressure–angle limited criteria do not apply.

5. STABILITY OF SESSILE DROPS

From earliest times it has been recognized that sessile drops resting on an infinitely large flat uniform horizontal surface are always stable. It is also well known that a sessile drop resting on a circular horizontal disk is only stable when the volume is relatively small. As the volume is increased, a point is reached where a part, if not all, of the liquid 'pours' over the edge of the disk. We believe the onset of this instability is of the same nature as that of the pendant drop and accordingly shall analyse for critically stable conditions.

Here we consider the stability of the four different types of system shown diagrammatically

in figure 6. The designations, stability criteria and conditions are the same as with pendant drops and thus are given in tables 1 and 2.

The evidence that $dV/d\beta$ (or $dV/d\phi$) is zero and the equilibrium volume reaches a maximum at critical equilibrium again relies on the solution of the variational problem concerning the relations between the energy of the sessile drop with its volume, the plate size, and the degree of perturbation from the equilibrium state. In figure 18 we present a three dimensional plot of the energy profiles of volume-radius limited sessile drops as a function of both volume and degree of perturbation. As pointed out in the introduction the degree of perturbation may be represented in a variety of ways. Here we have found that the use of ϕ, the angle of the meniscus at the plate, separates the maximum and minimum equilibrium points on the curve more conveniently than does Zg/k used in figure 3. As with figure 3, it is immediately obvious that a maximum equilibrium volume is reached when at critical conditions

$$(d^2W/d\phi^2)_{T\,V,X,k} = 0.$$

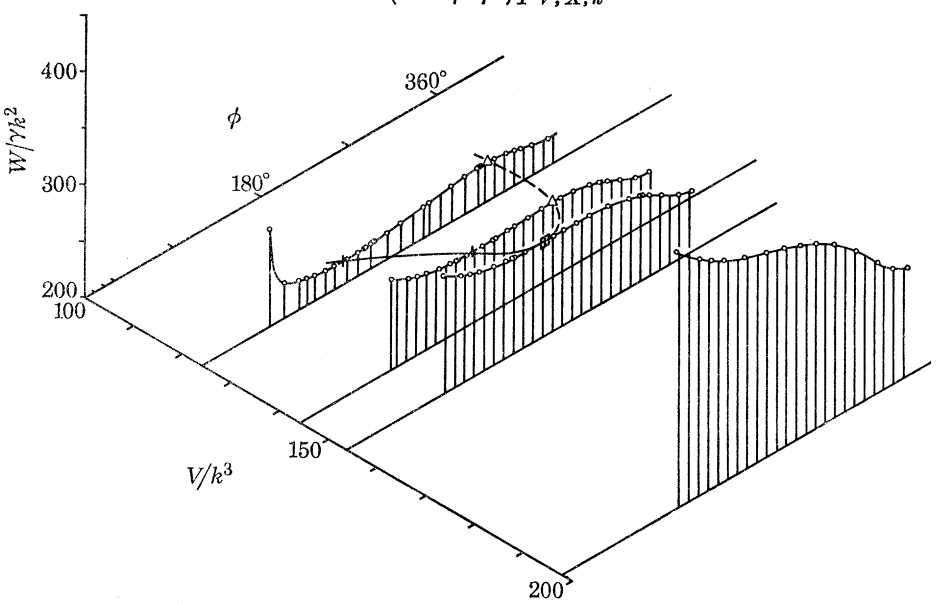

FIGURE 18. Sessile-drop stability: energy profiles of a volume–radius limited drop as a function of drop volume: +, points at stable equilibrium; △, points at unstable equilibrium; ⊞, point at critical equilibrium; ○, points that are unstable and not at equilibrium. $X/k = 4.6316$.

Unlike the pendant drop, a sessile drop's stability is very sensitive to the angle of the plate or disk supporting it. Whereas a pendant drop shows its characteristic shape when the tip is completely wetted and a small variation in ϕ of a stable drop, does not lead to instability, the sessile drop only obtains its characteristic shape when its contact angle is large, as with poorly wetted surfaces of low adhesion. The large contact angle coupled with the very much shallower energy trough of the stable system, leads to an instability that may be initiated by vibration or by the plates not being level. Experimentalists know only too well the difficulties of controlling the position of large sessile drops.

In figure 19 the profiles of a sessile drop in its unperturbed and perturbed form are shown. Shape C represents the stable equilibrium profile at $\beta = 3750$. It represents a fairly large drop with a meniscus angle of 180°. Perturbations that reduce this angle tend to reduce the value of β and raise the centre of gravity of the drop: these perturbations always result in free energy

increases. Perturbations that increase the angle of the meniscus change its shape so that the drop overhangs the plate to an ever increasing degree. When the unstable equilibrium state is reached any further change results in irreversible breakaway.

At critical stability the energy barrier between the stable and unstable states again reduces to zero and maximum drop-volume is reached.

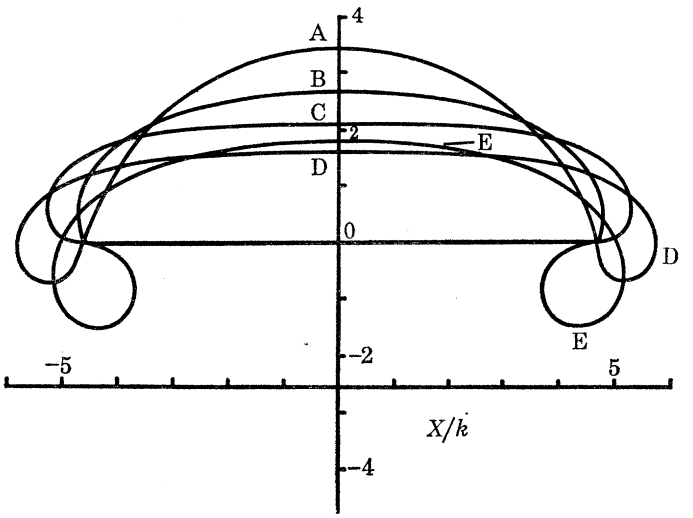

FIGURE 19. Perturbated shapes of a volume–radius limited sessile drop: A, $\beta = 1.0$; B, $\beta = 100$; C (stable equilibrium), $\beta = 3750$; D, $\beta = 3750$; E, $\beta = 100$; $V/k^3 = 144.2$; $X/k = 4.6316$. (These shapes are those relating to profile 2 of figure 18).

Volume–radius limited sessile drop

The critical stability conditions of this system (figure 6(i)) were obtained by the envelope construction method.

In figure 20 the volume of a sessile drop is plotted as a function of X/k. In order to demonstrate certain linear properties of the critical volume we have expressed the volume as its square root $(V/k^3)^{\frac{1}{2}}$. The lower part of the main curve is also plotted on an expanded scale to help with interpolation at small values of X/k.

Though we have not shown complete generating curves, the volume properties of a drop at constant X/k show a clearly defined maximum and again an envelope curve may be drawn. Each curve crosses every other curve, thereby indicating, as before, that a stable and unstable equilibrium state exists for each value of X/k and of V/k^3. Only small portions of each volume curve are shown for the sake of clarity, hence few intersections are actually seen. The volume of the critically stable meniscus divided by the plate radius cubed is plotted as a function of X/k on logarithmic scales in figure 21, covering a very much wider range of plate radii. As with figure 10 for the pendant drop, this plot is often more useful than figure 20, for interpolation of experimental results.

When the plate radius X/k is very small the critical angle of the meniscus approaches 270° and the total force supporting the volume V is given approximately by

$$2\pi X\gamma = \rho g V$$

or

$$V/Xk^2 = 2\pi \qquad (30)$$

When $X/k < 0.2$, equation (30) fits the slope and intercept of figure 21 with remarkable accuracy.

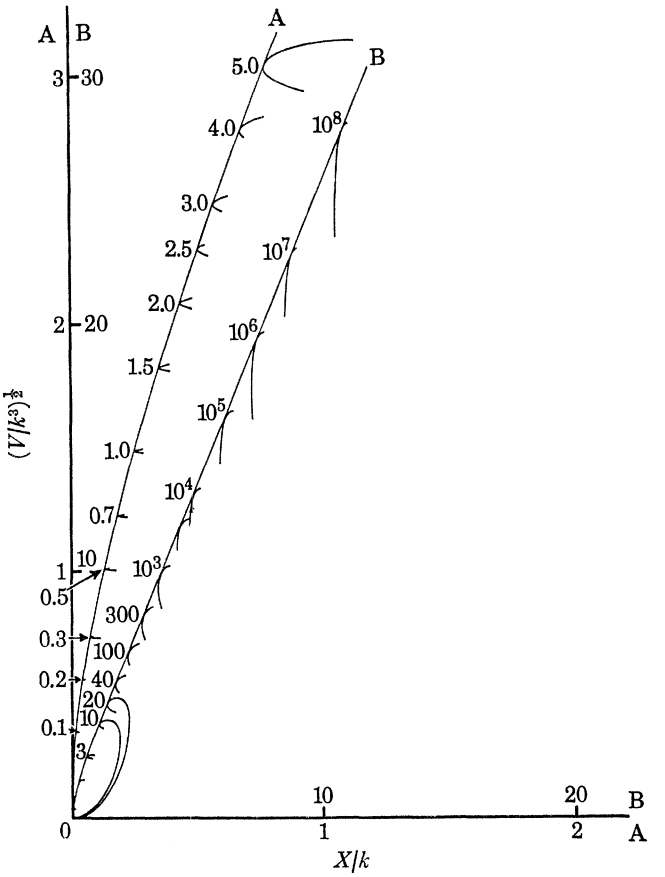

FIGURE 20. Sessile-drop stability, volume, expressed as $(V/k^3)^{\frac{1}{2}}$, of a drop as a function of plate radius; the envelope curves are the critical volumes as a function of plate radius. Shape factors β are shown for most profiles.

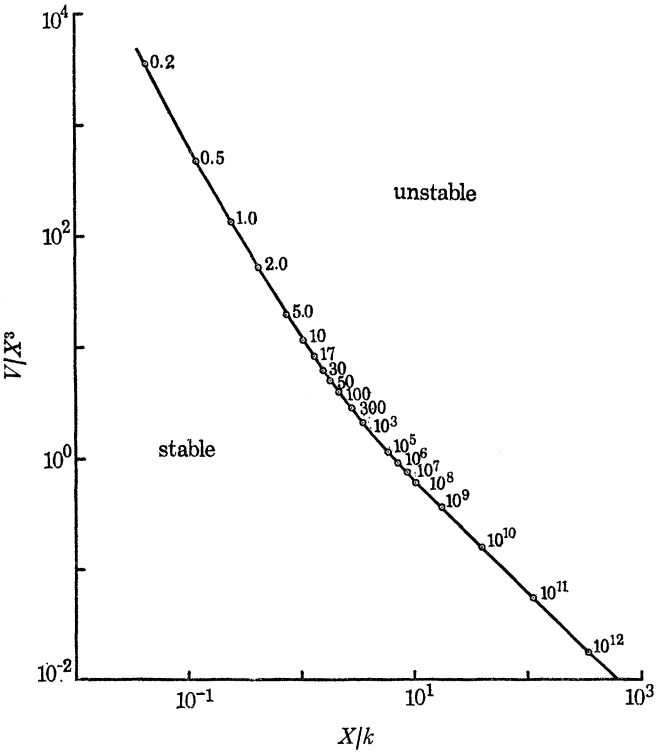

FIGURE 21. Sessile-drop stability: critical volume ratio, V/X^3 of a volume–radius limited drop as a function of plate radius. β values are indicated.

When the plate is large the critical angle of the meniscus approaches 180° and the volume of liquid approximates to that of a disk of height Z, where

$$\rho g Z^2/2 = 2\gamma \quad \text{or} \quad Z^2/k^2 = 4. \tag{31}$$

The volume V of a large drop approximates to that of a disk so that

$$V \approx \pi X^2 Z = 2\pi X^2 k \tag{32}$$

or

$$(V/k^3)^{\frac{1}{2}} \approx (2\pi)^{\frac{1}{2}} X/k, \tag{33}$$

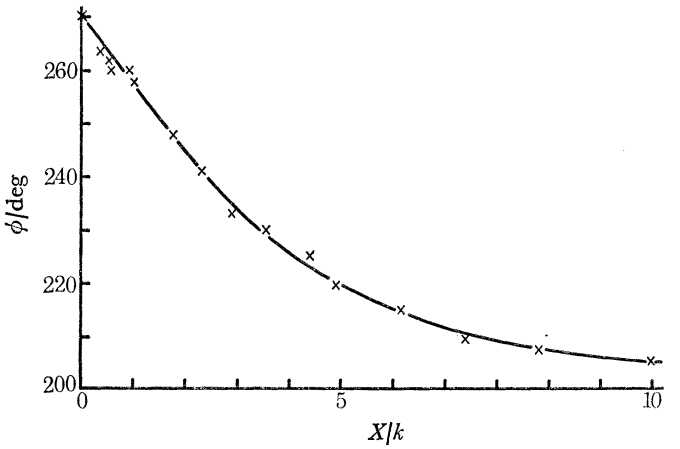

FIGURE 22. Sessile-drop stability: critical meniscus angle of a volume–radius limited drop as a function of plate radius.

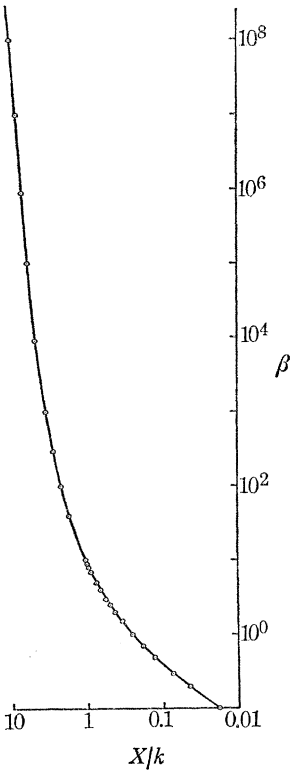

FIGURE 23. Sessile-drop stability: critical shape factor of a volume–radius limited drop as a function of plate radius.

which fits the plot of figure 20 with very good accuracy when $X/k > 2.0$. The upper limiting straight line portion of figure 20 is seen equally well by the corresponding linear portion of the plot of figure 21. In the intermediate section of figure 21 the meniscus angle for critical conditions varies between 180 and 270° in the way shown in figure 22.

Interpolation of the critical angle proved to be a difficult procedure, and this is reflected in the scatter of the data. The main point of this figure is that as the plate increases in size so the degree of overhang becomes smaller and smaller. Thus a large sessile drop rolling towards the edge of a flat plate will tend to 'pour' over the edge as soon as it is reached. The shape factor β from which these data have been derived is plotted as a function of X/k in figure 23. The plot is particularly helpful in interpolating data between the limits of application of equations (30) and (33).

Sessile drops, in general, tend to pour over the edge of the disk and, because of the low adhesion between liquid and the supporting plate already referred to, tend to leave no liquid behind once they have reached the critical conditions.

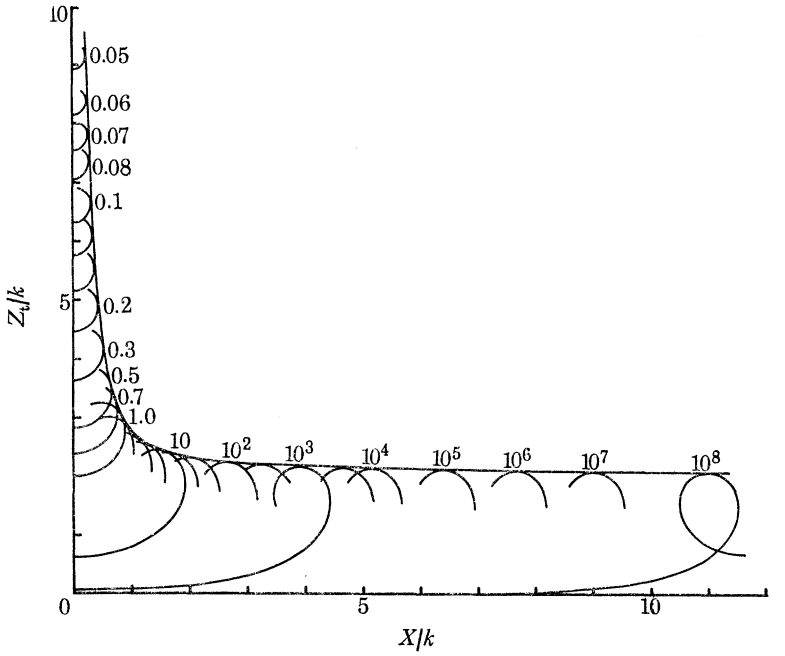

FIGURE 24. Sessile-drop stability; pressures of a captive bubble as functions of plate radii. The envelope curve is the critical pressure of a pressure–radius limited sessile drop, β values indicated.

Pressure–radius limited sessile drop

Let a pressure head be connected to the solid–liquid interface of a sessile drop in the manner indicated in figure 6 (ii) but in such a way that the hydrostatic pressure may be varied at will. The pressure is successively increased from zero and the volume builds up towards some critical value at which point dZ_t/dV and $dZ_t/d\beta$ become zero. At this point the pressure is a maximum, and further increases in the volume of the drop take place in an uncontrolled manner until the volume–radius limited maximum is reached, when the drop falls away.

The maximum pressure at the level of the plate was again obtained by the envelope construction method in figure 24. It is, of course, clear that the sessile drops of this figure are plotted as captive bubbles and that they are drop profiles positioned from the free surface according to

the value of Z_0, the hydrostatic height at the apex. At the critical pressure drops on plates of small radius take on a nearly hemispherical shape with $\phi \simeq 90°$. Drops on very large plates reach critical pressure conditions when ϕ approaches 180°, at which point the pressure–radius limited critical shape becomes equal to the volume–radius limited shape. Under these conditions the shape of the drop is that of a cylindrical meniscus.

The enveloping curve of figure 24 is generally hyperbolic and may be represented, when $X/k < 0.4$, by

$$Z_t X/k^2 = 2, \tag{34}$$

which follows from the Laplace equation applied to a hemisphere resting on a very small plate. For very large plates, i.e. when $X/k > 4.0$,

$$(Z_t/k - 2)\, X/k = 0.60. \tag{35}$$

Equation (35) is very similar in nature to the expression developed by Rayleigh (1915) and its modified form (Padday & Pitt 1972), for the pressure at the base of a sessile drop.

The pressure–radius limited sessile drop was investigated experimentally by Dupré as reported by Bouasse (1924). Their equation approximates to equations (34) and (35) at limiting conditions.

Volume–angle limited sessile drop

The most common and widely investigated axisymmetric meniscus is that of the volume–angle limited sessile drop shown in figure 6 (iii). The equilibrium of sessile drops of this type has been the subject of some speculation (Pethica & Pethica 1957), though in fact the equilibrium thermodynamics has been treated rigorously by Johnson (1959) using the virtual work principle.

The analysis from these tables, the work of Johnson, and simple observations, all indicate that sessile drops of this type are always stable. The volume of the sessile drop may increase indefinitely without any approach to a critical state. Thus all volume–angle limited sessile drops are stable and as such are very useful for observing the angle of contact between the liquid and the solid.

Pressure–angle limited sessile drop

The system shown in figure 6 (iv) is the pressure–angle limited system. It can never be realized experimentally as drawn, because it cannot attain stable equilibrium.

Like the corresponding pendant drop system the first stage of meniscus formation takes place at the orifice in the plate and growth is governed by the orifice radius and the hydrostatic pressure. The sessile drop increases in size as the pressure is raised, until the meniscus angle reaches the value of the contact angle. At this point, the drop spreads out over the flat solid surface, and in so doing the pressure due to Laplace curvature diminishes. This diminution in pressure results in instability. The critical stability point is reached either at the envelope curve of figure 24 or at the point at which the meniscus angle ϕ equals the contact angle – whichever comes first.

6. Stability of rod-in-free-surface menisci

The rod-in-free-surface meniscus (r.i.f.s.) is formed when a wetted rod is withdrawn from a free surface of a liquid and also when an unwetted disk is pressed below a free surface. Four of the more common types that are studied here are shown in figure 7. These menisci possess the common property of being bounded by the free flat surface of the liquid. The unwetted disk

produces a meniscus shape exactly similar to that of the rod, but with the difference that the meniscus appears as a hole in the surface and its profile appears as a reflected image of that at the rod.

The r.i.f.s. meniscus is formed by immersing the end or tip of a rod in the surface of a liquid just enough to ensure good wetting. The rod is then raised vertically so that it is above the general liquid level, as shown in figure 7. At first stable menisci are formed, but as the rod is further raised the degree of stability decreases until at a critical height the liquid bridge breaks away.

Unlike the pendant and sessile drops, r.i.f.s. menisci reach a maximum volume before attaining the limiting height of the critically stable condition. Freud & Freud (1930) recognized this in their treatment of the Du Noüy ring meniscus. The maximum pull on the rod, equivalent to that of the maximum volume of the meniscus is a property of considerable importance, but as it is not directly related to stability properties it will not be considered here.

In principle, the same methods for obtaining the criteria for critical stability apply and these criteria are set out in table 3. Again tabular interpolations and the envelope construction method were used to obtain data for critical conditions of the r.i.f.s. menisci.

TABLE 3. STABILITY CRITERIA FOR ROD-IN-FREE-SURFACE MENISCI.

	stable equilibrium	critical equilibrium	unstable equilibrium
(i) Volume–radius limited (X, X_D and k constant)	$\frac{dZ_t}{d\beta'} < \frac{dV}{d\beta'}\frac{1}{\pi X_d^2}$	$\frac{dZ_t}{d\beta'} = \frac{dV}{d\beta'}\frac{1}{\pi X_d^2}$	$\frac{dZ_t}{d\beta'} > \frac{dV}{d\beta'}\frac{1}{\pi X_d^2}$
(ii) pressure–radius limited (X and k constant)	$\frac{dZ_t}{d\phi} < 0$	$\frac{dZ_t}{d\phi} = 0$	$\frac{dZ_t}{d\phi} > 0$
(iii) Volume–angle limited (θ, X_D and k constant)	$\frac{dZ_t}{d\beta'} < \frac{dV}{d\beta'}\frac{1}{\pi X_d^2}$	$\frac{dZ_t}{d\beta'} = \frac{dV}{d\beta'}\frac{1}{\pi X_d^2}$	$\frac{dZ_t}{d\beta'} > \frac{dV}{d\beta'}\frac{1}{\pi X_d^2}$
(iv) pressure–angle limited (θ and k constant)	not met	not met	$\phi - 180 > \theta$

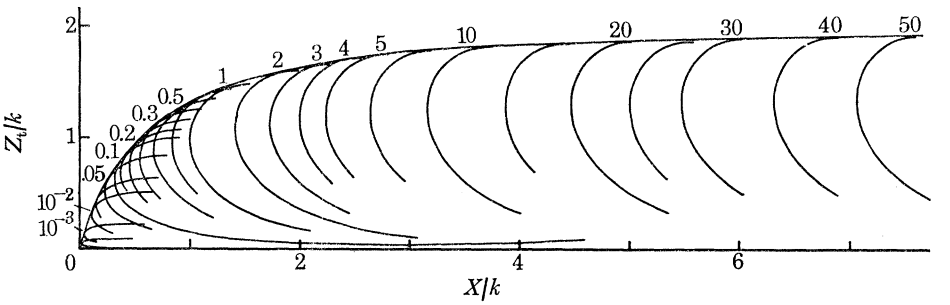

FIGURE 25. R.i.f.s. meniscus stability: pressure of a pressure–radius limited meniscus as a function of rod radius. The envelope curve is the maximum or critical pressure function. Shape factors, β', are shown for most profiles.

Pressure–radius limited r.i.f.s. menisci

In this system (figure 7 (ii)) it will be assumed that the tip of the rod is completely wetted and that the contact angle is 0°. We have obtained energy profiles for this type of meniscus, the same in character as those for the pendant and sessile drops. They are not presented here as they do not show any new features.

The condition for stability is represented by the maximum height above the free surface, i.e. the maximum pressure at the tip. This height, Z_t/k, is expressed as an envelope function of

X/k in figure 25 by plotting the profiles given by successive shape factors. As in previous work (Padday 1971) the shape factor, β', of an r.i.f.s. meniscus is defined as

$$\beta' = \rho g R_h^2(270°)/\gamma. \tag{36}$$

$R_h(270°)$ is the horizontal radius of curvature at the thinnest part of the neck. Although the complete profile at each β' value is not drawn, it is clear that each curve again intersects every other, each pair intersecting only once within the envelope. Thus for a given value of X/k, and a value of Z_t/k below the critical value, two shapes are possible, those corresponding to the stable and the unstable equilibria. The profile with the larger value of β' represents the stable equilibrium shape, and that with the smaller value the unstable equilibrium shape. As with energy profiles of pendant drops, the difference in energy between the stable and unstable state may be regarded as a measure of the degree of stability.

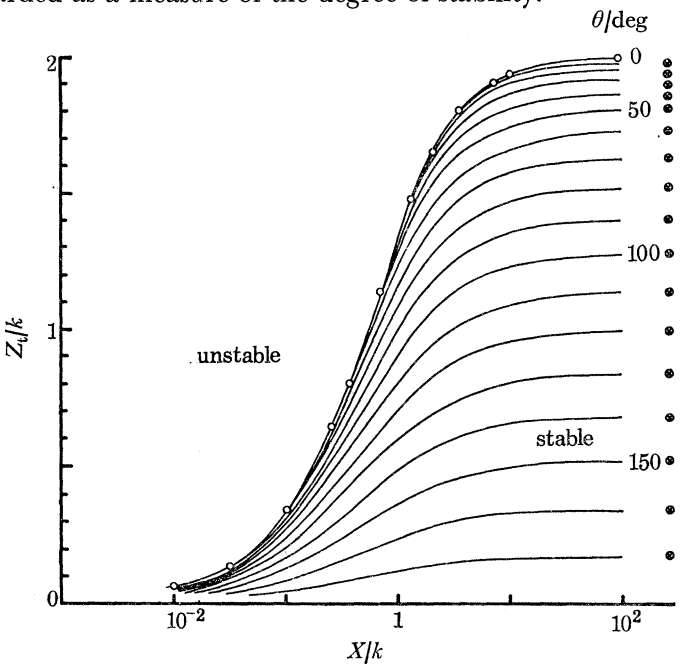

FIGURE 26. R.i.f.s. meniscus stability: critical pressure of a pressure–radius limited meniscus as a function of rod radius. The function (○) is for contact angle $\theta = 0°$. Other curves represent critical conditions when the stability is limited by the value of θ (indicated). ⊗, limiting values for very large drops.

The data of figure 25 cover only a small range of X/k. A much wider range has been plotted logarithmically in figure 26. The envelope curve of figure 25 is represented by the curve at $\theta = 0°$ on figure 26.

The critical height of profiles formed with very large rods approaches the limiting value of that of a cylindrical meniscus. This height, Z_t, thus becomes equal to the limiting height of a sessile drop (Padday & Pitt 1972). Substituting Z_t in the sessile drop equation gives

$$\rho g Z_t^2 = 2(1 - \cos\phi). \tag{37}$$

When $\phi = 180°$,

$$Z_t/k = 2. \tag{38}$$

The meniscus angle, ϕ, of the r.i.f.s. is not equal to the angle of contact, θ, of the liquid to the horizontal solid. Instead, figure 7 (iii) shows that

$$\phi - 180 = \theta. \tag{39}$$

An important feature of pressure–radius limited r.i.f.s. menisci is that the critical meniscus angle ϕ varies between 180° for very large rods and 270° for very small rods. The value of ϕ for critical conditions is plotted as a function of X/k in figure 27. The plot shows, for instance, that the meniscus formed by a wetted rod of 2.5 cm radius receding from water ($k = 0.27$) would reach critical conditions when $\phi = 180°$, but remains stable when $\phi = 185°$. With smaller rods, $X/k < 0.01$ the menisci appear to reach a limiting value between 255° and 260°. This latter point requires confirmation as our errors are rather larger than average in this region.

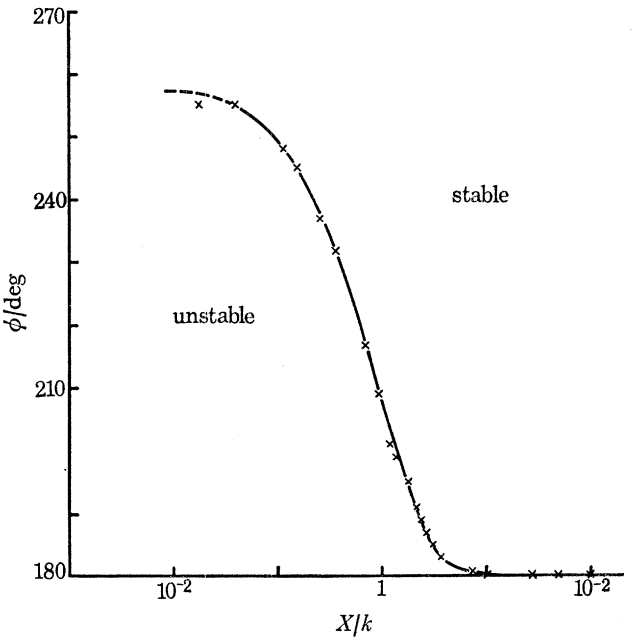

FIGURE 27. R.i.f.s. meniscus stability: critical meniscus angle of a pressure–radius limited meniscus as a function of rod radius.

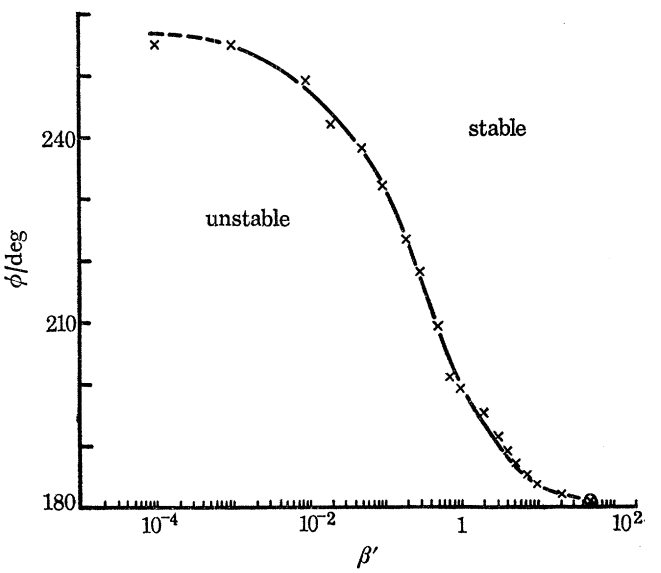

FIGURE 28. R.i.f.s. meniscus stability: critical meniscus angle of a pressure-radius limited meniscus as a function of the shape factor β'.

The meniscus angle, ϕ, for critical conditions is also related to the shape factor, β', in a manner similar to that with X/k. The critical angle of the pressure–radius limited r.i.f.s. meniscus is plotted as a function of log β' in figure 28. At critical equilibrium any perturbation of the system to a lower meniscus angle or lower shape factor results in instability and rupture. However, corresponding increases in either ϕ or β' results in the meniscus becoming transiently stable.

Experimentally one measures both the rod radius X, and the limiting height Z_t reached at critical conditions, k being unknown. Providing the tip is completely wetted, X/k may be found from the ratio Z_t/X in the $\theta = 0-30°$ curve of figure 29; hence k is derived.

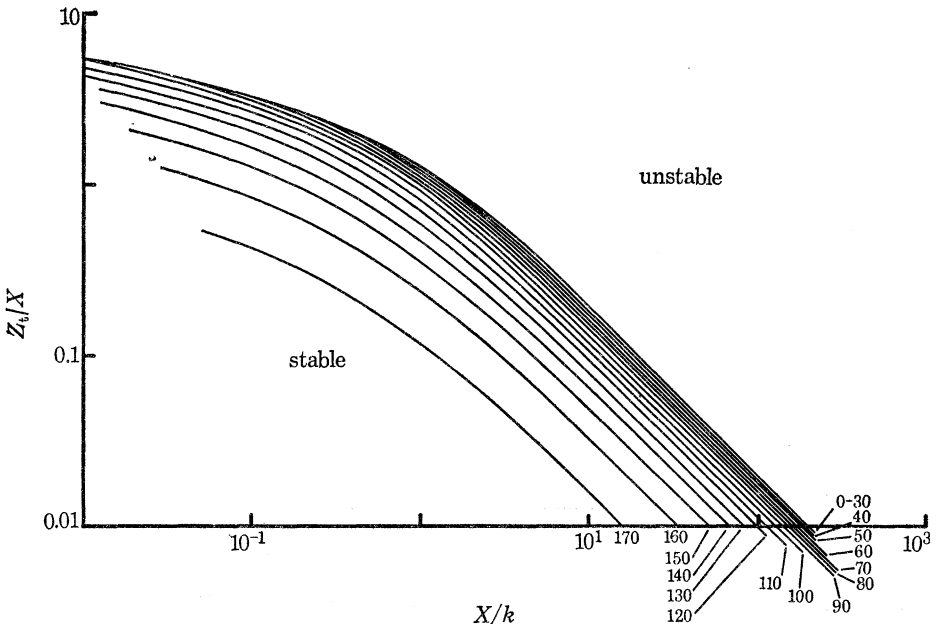

FIGURE 29. R.i.f.s. meniscus stability: critical pressure ratio of a pressure–radius limited meniscus as a function of the rod radius. The function is for contact angle $\theta = 0$–$30°$. Other curves represent critical conditions when the stability is limited by the value of θ (indicated).

Pressure–angle limited r.i.f.s. menisci

The criterion for stability and for critical conditions radically changes when the liquid forms a finite angle of contact with the undersurface of the rod as shown in figure 7 (iv).

Consider a plate, the radius, X/k, of which equals 2.0, and possessing a contact angle, θ, of 50° with the liquid which it is about to support. The plate is now lowered so that it just touches and is wetted by the free surface of a liquid. The effective meniscus angle, ϕ, as defined in figure 7, assumes a value of 360°. The plate is now raised slowly so that a meniscus is formed between its edge and the free surface, and the meniscus angle decreases from 360° towards the value 192°. However, equation (39) shows that the contact angle limits the meniscus angle to a value of 230°. At a certain stage in raising the plate the meniscus angle reaches 230°, and further movement causes the meniscus to recede on the underside of the plate. Recession of the meniscus results in a diminution of both X/k and the critically stable value of Z_t/k (figure 26). The drop in pressure inside the liquid at the underside of the plate results in further recession until the liquid bridge breaks away. The condition of critical stability of the pressure–angle limited system is thus reached when the meniscus angle reduces to the value specified by equation (39).

The parameters for critical stability of an r.i.f.s. meniscus limited by contact angle are best represented as a further restriction on the pressure–radius limited r.i.f.s. data already presented. The critical data are shown in figure 26 where Z_t/k is plotted as a function of X/k for contact angles at 10° intervals between 0 and 180°. These data were extracted directly from the tables.

As before, the ratio Z_t/X has been plotted as a function of X/k for the contact angle limitation in figure 29. The main point to emerge from these data is that the meniscus as drawn in figure 7 (iv) is always unstable; it must either move outwards to the edge of the plate or inwards and then break away. The true critical stability represented by these data is rather a restriction on the pressure-radius limited data.

Volume–radius limited and volume–angle limited r.i.f.s. menisci

The r.i.f.s. menisci considered so far are of the type where the volume of liquid displaced from the free flat surface is very small compared with the liquid forming the whole system. In many experimental set-ups a reservoir sufficiently large is impossible to obtain, hence the total volume of liquid in the system is limited, as shown in figures 7 (i) and 7 (iii). The constant volume of these systems places a severe restriction on them and it is found both experimentally and from general theoretical considerations that a restricted volume increases the stability of an r.i.f.s. meniscus.

In order to treat the volume restriction in a simple way we introduce the term 'excluded volume', V_e, which is defined as the volume of vapour bounded by the liquid–vapour interface, the horizontal plane of the rod or plate, and the sides of the dish of radius X_d. It follows that

$$\pi X_d^2 Z_t - V_e = V. \tag{40}$$

By differentiating equation (40) with respect to a small perturbation in β' at constant total volume of liquid in the system we obtain

$$(\mathrm{d}Z_t/\mathrm{d}\beta')_{T, X_d, k, X \text{ or } \phi} = \mathrm{d}V_e/\pi X_d^2 \mathrm{d}\beta' + \mathrm{d}V/\pi X_d^2 \mathrm{d}\beta'. \tag{41}$$

Equation (41) is applied at constant k, X_d and ϕ or X. For conditions of critical stability we find the excluded volume, V_e, reaches a maximum value so that for small perturbations, $\mathrm{d}V_e/\mathrm{d}\beta' = 0$. This is because the change in meniscus volume exactly equals the change in volume below the free surface of liquid in the dish. (Note that the free surface rises or falls with the perturbation.) At critical stability

$$(\mathrm{d}Z_t/\mathrm{d}\beta')_{T, X_d, k, X \text{ or } \phi} = \mathrm{d}V/\pi X_d^2 \mathrm{d}\beta', \tag{42}$$

which is the condition given in table 3 when V_e has attained its maximum value. If the l.h.s. of equation (42) is greater than the r.h.s. the menisci of figures 7 (i) and 7 (iii) are unstable and if less, then they are stable. The difference is equal to the term $\mathrm{d}V_e/\pi X_d^2 \mathrm{d}\beta'$ in equation (41).

Systems limited by volume can be either angle limited, figure 7 (iii), or radius limited, figure 7 (i), but with the restriction that the volume of liquid is limited by the size of the dish.

We consider first the angle limited r.i.f.s. meniscus as it is somewhat simpler to understand. Only large rods are considered, and circular dishes such that $X_d/k > 10$. Also the angle of the free flat surface to the walls of the dish is always regarded as being 90°. To produce the meniscus the rod is withdrawn from the liquid as with the other r.i.f.s. systems. As the rod is raised the meniscus forms at the edge of the rod and the meniscus angle, which starts at 360°, diminishes toward 180°. At some stage of withdrawal the rod will become limited by the contact angle according to equation (36), and the meniscus will recede at the under surface of the tip.

However, the meniscus will not necessarily recede to the point at which it breaks away as happened with the corresponding meniscus at a semi-infinite surface, because the very process of receding decreases the volume in the meniscus, which in turn raises the level of the free flat surface in the dish.

The point of critical stability is reached when equation (42) holds. We have analysed the tables for four contact angle conditions, 0, 45, 90 and 135° and have found it easiest to express the results either as excluded volume plotted against dish radius (figure 30), or as critical height against dish radius (figure 31). The slope of the double logarithmic plot of figure 30

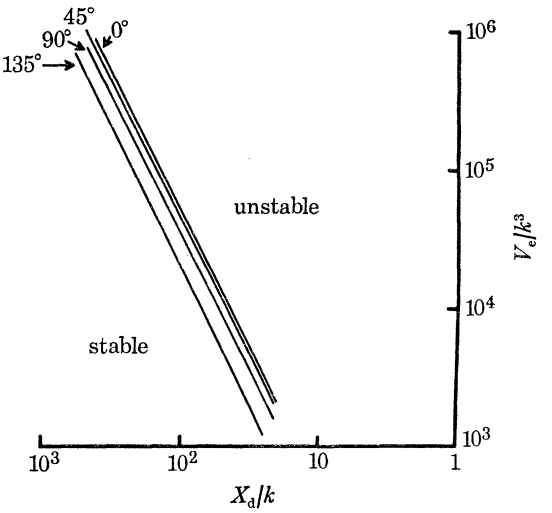

FIGURE 30. R.i.f.s. meniscus stability: critical or maximum excluded volume of a volume–angle limited meniscus as a function of dish radius. Limiting contact angles are indicated.

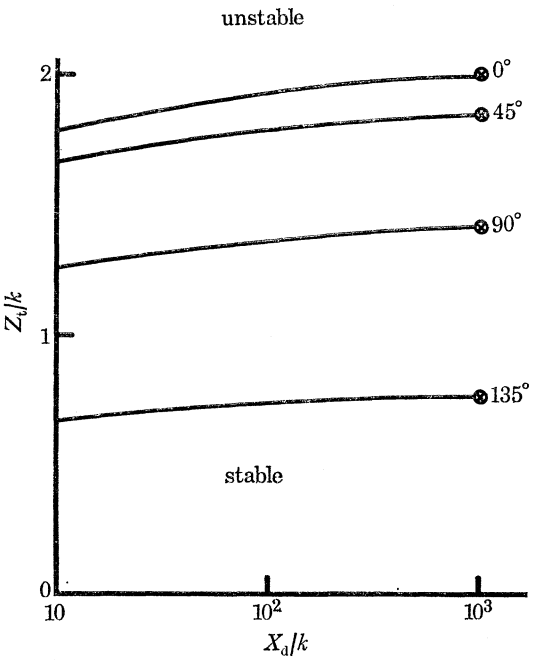

FIGURE 31. R.i.f.s. meniscus stability: critical meniscus height of a volume–angle limited meniscus as a function of dish radius for angles of contact indicated.

demonstrates clearly the square relation of equation (40) since under these conditions V is small compared with V_e. The main feature of the data of figures 30 and 31 is that even very large containers completely alter the nature of the stability and change it from pressure limited to volume limited conditions. For this reason it is very unusual to find experimental conditions under which the stability of the system of figure 7 (ii) can be studied.

In order to interpolate for angles of contact between those plotted in figure 30 we have assumed linearity at all other angles and have plotted in figure 32, the intercept X_d/k with the line $V_e/k^3 = 10$ of figure 30 as a function of the cosine of the contact angle. The linear plot then enables all other critical excluded volumes to be derived provided that the contact angle is known. The meniscus heights of figure 31 are used experimentally and show that for a large dish the height approaches the limiting height set by equation (37).

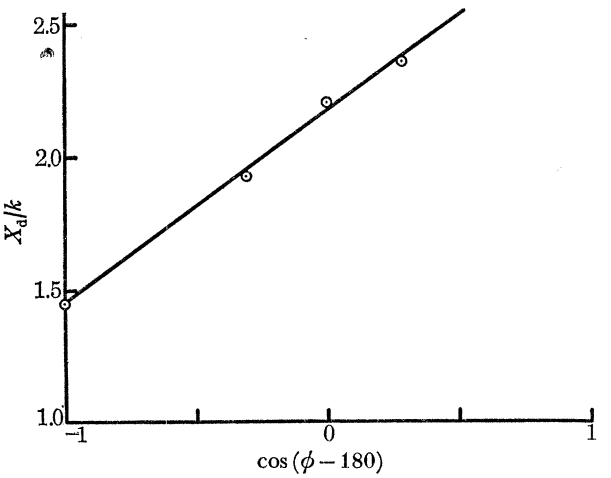

FIGURE 32. R.i.f.s. meniscus stability: dish radius of a volume–radius limited meniscus as a function of cos (ϕ – 180), where ϕ is the critical angle of the meniscus. Data for $V_e/k^3 = 10$.

The volume–radius limited r.i.f.s. meniscus of figure 7 (i) is in fact only a special case of the volume–angle limited system. If the rod radius X/k is relatively small, then on raising the rod from the dish of liquid as in figure 7 (i) critical conditions are reached before the meniscus angle reaches the contact angle condition of equation (39). The critical stability criterion of such a system is given in table 3, but in experimental systems involving very small rods the pressure–radius limited data of figure 26 provide accurate results. For larger rods no data are given because the complex calculation procedure hardly merits the value of the results obtained. Such systems are more appropriately treated as liquid bridges.

7. DISCUSSION

In this study we have set out in thermodynamic terms the Helmholtz free energy or work of formation of a bounded meniscus in a gravitational field; defined the stable, unstable and critical equilibrium states of bounded menisci; shown that the three main types of menisci may have their stability conditions limited by volume or by pressure; analysed the variational problem graphically and shown that a measurable parameter takes on a maximum or minimum value at critical conditions; and presented numerical values of a wide range of meniscus properties for critically stable conditions of twelve different systems.

The determination of critical conditions involves certain new approaches, the most important of which are the construction of energy profiles by using equilibrium tables in a 'non-equilibrium' way and the demonstration of a solution to the variational problem by graphical analysis.

The thermodynamic statements in the introduction are applicable to systems only where the liquid and vapour phases are of a single component. The form of the thermodynamic equations deviates from the usual treatments in that we have included external energy with the surface free energy, following Everett & Haynes (1972). The equilibrium of a system is thus one which the variations of the areas of the meniscus and of the potential energy due to raising or lowering the centre of gravity, at constant temperature, k, and p, are the only contributions to the free energy.

Justification of our hypothesis that axisymmetric perturbations of this study are those of lowest energy rests first on the fact that breakaway, in the absence of extraneous sideways forces, always occurs with axial symmetry. Secondly the change in pendant drop shape that does occur in the early stages of breakaway appears to follow the shapes dictated by the energy profile for the critical conditions such as that seen in figure 3. At later stages of breakaway potential energy is lost by the system irreversibly and the drop accelerates away from the tip in a manner dictated by kinetic and viscosity factors.

In two previous studies (Erle, Dyson & Morrow 1971; Erle, Dyson & Gillette 1970) the gravity-free stability of liquid bridges has been investigated by variational analysis. Their results represent the alternative volume-limited condition and not Plateau's pressure-limited condition, applied to soap films. Also their results are not comparable with the work of Lohnstein (1906, 1907*a*, *b*), who like us, studied the equilibrium and stability of drops in a gravitational field.

The graphical analysis of this study enables one to derive the properties of a meniscus in its critical state and it shows clearly that the intuitive step of Lohnstein (i.e. that maximum volume is reached at the critical condition) was correct (figure 3). We have further found that the method used by Lohnstein for calculating the maximum volume (using a truncated series expansion of $\sin\phi$) is sufficiently accurate for many experimental purposes.

In figure 33 the critical volumes of a pendant drop obtained from our data, together with Lohnstein's results, are plotted as a function of tip radius. The deviation between the two results is less than 1 %. It may be seen too that Tate's law,

$$V/k^3 = 2\pi X/k, \tag{43}$$

is only approximate to $\pm 18\,\%$ and then only when $X/k < 3.2$, and measures only the critical volume and not the amount of liquid falling away as Tate had supposed.

Lohnstein also noted that when the critical meniscus angle of a pendant drop reached 0°, a maximum value of 18.84 for V/k^3 was reached. We confirm this maximum value (but with a revised value of 18.88) by providing data for the 'bath tap' type or critical stability of figure 9, obtained when $X/k > 3.2$. We suggest designating this maximum volume situation, $\phi = 0°$, as the '*Lohnstein point*' in recognition of his correct predictions (without the aid of modern computers). The Lohnstein point also appears on the critical data of the volume–angle limited pendant drop given in figure 16, showing that the drop at critical conditions, hanging from a ceiling, possesses this volume.

The tables and the integration procedure giving the basic data are accurate to $\pm 0.001\,\%$ (Padday 1971). However, this accuracy was not maintained in the data presented here because

interpolation procedures would have involved very long and hence costly computations. Instead we have adopted truncation procedures which have reduced the accuracy to $\pm 0.05\,\%$. However, we find that errors in interpolating angles was no better than $\pm 2°$ as may be seen in figure 22. But angles were not basic data, hence their inaccuracy did not impair the quality of the other data.

The r.i.f.s. volume-limited stability data were difficult to derive accurately because the envelope construction method could not be applied easily. We therefore present only outline data that give an insight into the problem and with sufficient accuracy ($\pm 1\,\%$) for general experimental work.

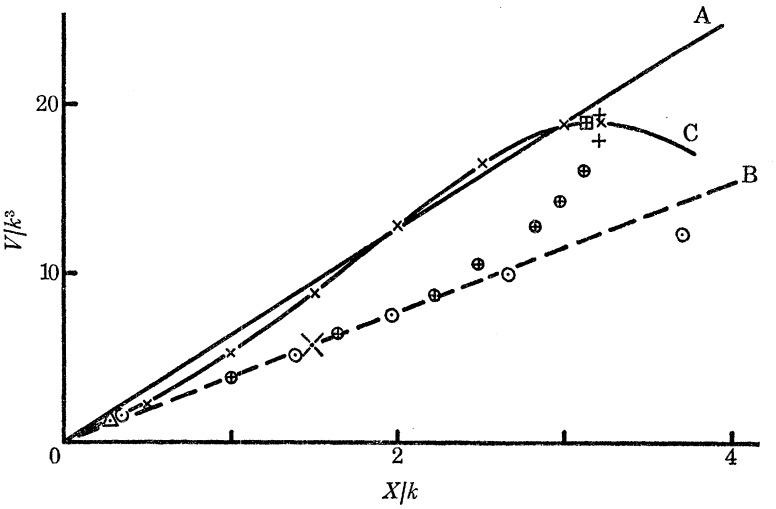

FIGURE 33. Comparison of critical and separating volumes of a volume–radius limited pendant drop as a function of tip radius. A, Tate's equation; B, Rayleigh's equation; C, this study; ×, Lohnstein's critical volumes; ⊕, Lohnstein's separating volumes; ⊞, the Lohnstein point; ⊙, Harkins & Brown's drop volumes; ⋇, Picknett's separating volume; △, Izard's separating volume, C_6H_6—H_2O; +, Halligan & Burkehart's critical volumes.

The analysis of this study is thus sufficiently precise to confirm that:

(i) At critically stable conditions, volume–limited menisci reach a maximum volume at Laplace equilibrium.

(ii) At critically stable conditions, pressure-limited menisci reach a maximum pressure at Laplace equilibrium.

These conclusions arise from the properties of the energy profiles and their variation with volume or pressure as shown in figures 3 and 18. In each profile we find that the points at Laplace equilibrium fall exactly at the bottom of the trough and at the crest of the hump.

In order to compare the theoretical results of this study with experimental data, one must recognize that the critical volumes of this study represent the total volume of the drop or meniscus before detachment and not the amount falling away. Also in real systems the actual critical point may never be reached if vibrations are allowed to perturb the system and initiate premature rupture. In figure 33 the 'drop-weight' volumes obtained experimentally by Rayleigh (1899) and by Harkins & Brown (1919) show clearly the difference between the critical volume and the amount falling away. Lohnstein attempted to calculate the amount left behind after breakaway, on the basis that the meniscus angle of the remainder was the same as that of the critical pendant drop. This supposition is surprisingly good when $X/k < 2.0$

(figure 33) but only holds at low viscosity. The drop volume falling away is thus reasonably predicted by Rayleigh's formula (Rayleigh 1899).

$$V/k^3 = 3.8X/k \tag{44}$$

for $$X/k < 2.5.$$

Picknett (1970) has made available the photographs of pendant drops just before rupture, and we find the experimental parameters of his critical shapes agree within $\pm 0.5\,\%$, with the values obtained theoretically here. His drop volume for the separating drop agrees well with other work as shown in figure 33.

The breakaway of pendant drops has received much attention recently, mainly from those studying the break-up of liquid jets. Among these Halligan & Burkhart (1968) used an empirical form of Bashforth & Adam's equation in order to calculate the profile of a separating droplet. Their results are plotted in figure 33 and indicate predictions of the critical volume (not the amount breaking away) with about 5 % error; in order to plot their data we have assumed their critical meniscus angle to be $\phi = 0°$.

Izard (1972) also studied the break-up of liquid jets emerging from a small unwetted orifice. His result for the benzene–water system extrapolated to zero flow has been plotted in figure 33 using the densities and interfacial tension values of Harkins & Young (1929). Their point lies on the curve of figure 33 in the region where the critical volume of the pendant drop meniscus is almost equal to the volume falling away. The difference between the critical volume of a pendant drop and the amount falling away is viscosity dependent, hence Harkins & Brown's data in figure 33 is only a special case for low viscosity liquids. Complete resolution of this difference must await a full kinetic analysis of the pendant drop breakaway once the critical volume is reached.

Experimental verification of the other eleven systems of this investigation is not yet complete. However, we have investigated experimentally the systems consisting of a rod drawn from a free surface (r.i.f.s.) and its corresponding mirror image, the hole in free surface, and we find from our limited number of experiments good agreement between theory and practice. However, experimental work will be reported separately.

It is believed that the critical data presented in this study have been compared with as wide a variety of data as we could find in the literature, and in no case have we been able to find disagreement other than that arising from normal experimental error.

The authors record their grateful thanks to Professor D. H. Everett, Dr T. D. Blake, Dr M. Haynes, Mr A. Marriage and Dr R. Picknett for the valuable and friendly discussions and are greatly appreciative to Dr Picknett for making available some of his unpublished results which appear in figure 33.

8. Appendix A. Identification of dW with the Helmholtz free energy dF

This treatment follows that of Gibbs (1906) and of Everett & Haynes (1972) and their further suggestions. The work done on the system by compressing the syringe isothermally and reversibly as in figure 1 is dW.

From the first law, the change in internal energy

$$dU = dW + dQ. \tag{1A}$$

The entropy change is given from the second law

$$\mathrm{d}S = \mathrm{d}Q/T + \mathrm{d}_{\mathrm{i}}S, \tag{2A}$$

where $\mathrm{d}_{\mathrm{i}}S \geqslant 0$ and ${}_{\mathrm{i}}S$ is the entropy arising from irreversible processes within the system.

The total internal energy change then is

$$\mathrm{d}U = T\mathrm{d}S + \mathrm{d}W - T\mathrm{d}_{\mathrm{i}}S. \tag{3A}$$

By differentiating the definitive equation for Helmholtz free energy

$$F = U - TS \tag{4A}$$

and combining this with equation (3A) we obtain

$$\mathrm{d}F = \mathrm{d}W - T\mathrm{d}_{\mathrm{i}}S - S\mathrm{d}T. \tag{5A}$$

At constant temperature T,

$$\mathrm{d}F = \mathrm{d}W - T\mathrm{d}_{\mathrm{i}}S. \tag{6A}$$

At equilibrium both $\mathrm{d}F$ and $\mathrm{d}_{\mathrm{i}}S$ equal zero, therefore

$$\mathrm{d}W = 0. \tag{7A}$$

For small departures from equilibrium, $\mathrm{d}F$ equals $\mathrm{d}W$ and the virtual work principle may be used to derive energy changes in the system because the term $T\mathrm{d}_{\mathrm{i}}S$ is vanishingly small. For larger deviations

$$T\mathrm{d}_{\mathrm{i}}S = T\mathrm{d}A(\mathrm{d}\gamma/\mathrm{d}T). \tag{8A}$$

However, the term $T\mathrm{d}_{\mathrm{i}}S$ is always small compared with $\mathrm{d}W$, hence

$$\mathrm{d}F = \mathrm{d}W \tag{9A}$$

for the perturbations of this study.

9. Appendix B. Method for calculating the energy profile of a bounded meniscus

1. Obtain a set of tables of axisymmetric meniscus profiles (Padday 1972). Alternatively computer programs may be used.
2. Define the value of k either by arbitrary choice, or from experimental values of ρ, g and γ.
3. Select the tables appropriate to the form of the bounded meniscus.
   - (a) Sessile drop.
   - (b) Pendant drop.
   - (c) Rod-in-free-surface.
4. Define two other experimental properties of the system. These properties are used to set the shape factor and the limit or boundary conditions of the equilibrium shape being sought in the tables and must remain constant.

The experimental properties of a meniscus from which two may be chosen are more usually:

(i) Volume of the drop or meniscus.
(ii) Angle of contact, θ, of the meniscus with the support.
(iii) The radius, X, of the solid surface supporting the meniscus.
(iv) The axial height, Z_{t}, of the free liquid level from the tip or the supporting surface of the meniscus.

5. Fix the values of the two chosen properties which limit the type of stability (e.g. for a volume–radius limited system fix V/k^3 and X/k).

6. Determine the shape factor β, $(\rho g b^2/\gamma)$, and hence the appropriate table in which the stable equilibrium is to be found. An approximate value of b, the radius at the lower extremity of the drop, is measured or obtained by regarding the drop as spherical so that $b = (3V/4\pi)^{\frac{1}{3}}$. This value gives an approximate shape factor and leads to the useful range of the tables.

The ratios of the experimental values, V/X^3 and X/k are used to find the equilibrium value of β and ϕ, by interpolation in the tables. Very often the equilibrium value of β lies between two tables, but simple scaling procedures enables one to estimate an accurate value.

7. Using the same interpolative procedures calculate the area of the pendant drop from the tables for this same condition.

8. Find the position of the centre of gravity, Zg, of the drop. This may be done with sufficient accuracy by first summing the products of the volume increment with the distance of the increment from the tip (at each 5° interval). The sum of the products is then the potential energy term of equation (9) and this when divided by the total volume gives the distance of the centre of gravity from the tip.

In the data of figures 2, 3 and 16 the potential energy and centre of gravity of each shape were obtained more accurately by carrying out the summation at every 0.025° intervals by means of a computer.

9. Calculate the total energy or work of formation of the meniscus from equation (9).

10. Obtain the energies of the meniscus in its perturbed shapes by choosing arbitrary shape factors slightly displaced from the equilibrium value. In each table we scan for one or possibly two values of ϕ where the value V/X^3 equals that of the experimental starting conditions. At this point of correspondence, X/k' in the tables does not equal X/k experimental, because the value of k' in the tables cannot be the same as the experimental value.

11. Define a magnification M by

$$M = (X/k \text{ (expt.)})/(X/k' \text{ (tables)}). \tag{1B}$$

12. Find in the tables the surface area and the position of the centre of gravity in the same manner as for the equilibrium point and the total energy of the perturbed state is now obtained from

$$W/\gamma k^2 = AM^2/k'^2 - VZgM^4/k'^4 - \pi X^2 M^2 \cos\theta/k'^2. \tag{2B}$$

13. Obtain further energy points using other tables (β values) so that finally the whole profile is obtained.

References

Bakker, G. 1928 *Handb. Exp. Phys.* IV, p. 113.
Bashforth, F. & Adams, J. C. 1883 *An attempt to test the theory of capillary action.* Cambridge University Press.
Bouasse, H. 1924 *Capillarité. Phénomènes superficiels*, Paris: Delagrave.
Brown, R. C. & McCormick, H. 1948 *Phil. Mag.* **39**, 420.
Buff, F. P. 1960 *Handb. Phys.* **10**, 281.
Erle, M. A., Dyson, D. C. & Gillette, R. D. 1970 *Chem. Engng J* **1**, 97.
Erle, M. A., Dyson, D. C. & Morrow, N. R. 1971 *A.I.Ch.E. Jl* **17**, 115.
Everett, D. H. & Haynes, J. M. 1972 *Z. phys. Chem. Neue. Folge* **82**, 36.
Freud, B. B. & Freud, H. Z. 1930 *J. Am. chem. Soc.* **52**, 1772.
Gibbs, J. W. 1906 *Scientific papers*, vol. 1. New York: Dover, 1961.
Gillette, R. D. 1970 Thesis: *The stability of axisymmetric fluid interfaces.* Houston: Rice University.
Halligan, J. E. & Agrawal, B. K. D. 1971 *Ind. Engng Chem. Fund.* **10** (4), 577.

PHILOSOPHICAL TRANSACTIONS OF THE ROYAL SOCIETY A MATHEMATICAL, PHYSICAL & ENGINEERING SCIENCES

Halligan, J. E. & Burkhart, L. E. 1968 *A.I.Ch.E. Jl* **14**, 411.
Harkins, W. D. & Brown, F. E. 1919 *J. Am. chem. Soc.* **41**, 503.
Harkins, W. D. & Young, T. F. 1929 *Int. crit. Tabl.* **4**, 436.
Hayworth, C. B. & Treybal, R. E. 1950 *Ind. Engng Chem.* **42**, 1174.
Izard, J. 1972 *A.I.Ch.E. Jl* **18** (3), 634.
Johnson, R. 1959 *J. phys. Chem.* **63**, 1655.
Laplace, P. S. de 1805 *Mécanique Celéste. Suppl. au Xe livre.* Paris: Courier.
Lohnstein, T. 1906 *Annln Phys.* **20**, 237, 606.
Lohnstein, T. 1907*a* *Annln Phys.* **21**, 1030.
Lohnstein, T. 1907*b* *Annln Phys.* **22**, 767.
Lohnstein, T. 1913 *Z. Phys. Chem.* **84**, 410.
Null, H. R. & Johnson, H. F. 1958 *A.I.Ch.E. Jl* **4** (3), 273.
Padday, J. F. 1971 *Phil. Trans. R. Soc. Lond.* A **269**, 265.
Padday, J. F. 1972 *J. electroanal. Chem.* **37**, 313.
Padday, J. F. & Pitt, A. 1972*a* *J. Colloid and Interface Sci.* **38**, 323.
Padday, J. F. & Pitt, A. 1972*b* *Proc. R. Soc. Lond.* A **329**, 421.
Pethica, B. A. & Pethica, T. J. P. 1957 *Proc. Int. Congress Surface Activity* (ed. Schulman), **3**, 131. London: Butterworth.
Plateau, J. 1873 *Statique expérimentale et théorique des liquides.* Paris: Gauthier-Villars.
Poutanen, A. A. & Johnson, A. I. 1960 *Can. J. chem. Engng* **38**, 93.
Rayleigh, Lord 1899 *Phil. Mag.* **48**, 321.
Rayleigh, Lord 1915 *Proc. R. Soc. Lond.* A **92**, 184.
Scheele, G. F. & Meister, B. J. 1968 *A.I.Ch.E. Jl* **14**, 9.
Tate, T. 1864 *Phil. Mag.* **27**, 176.
Young, T. 1804 *Miscellaneous works* (ed. G. Peacock), vol. 1, p. 419. London: Murray.

Symbols

A	area of liquid–vapour interface
A'	area of solid–liquid interface
A_0	area of liquid–vapour interface at beginning of drop growth
b	principal radius of curvature at apex of drop or bubble
C	constant of integration
d	differential quantity
F	Helmholtz free energy of a meniscus
$f_{1,2,3}$	functions
g	gravitational acceleration
k	meniscus coefficient, $(\gamma/\rho g)^{\frac{1}{2}}$ ($k' \equiv$ non-equilibrium value)
M	magnification factor
p	vapour pressure
PE	potential energy in relation to gravitational force
Q	energy supplied to the system
R_h horizontal, R_v vertical	principal radii of curvature
S	reversible entropy of meniscus formation
$_iS$	irreversible entropy of meniscus formation
T	absolute temperature
U	internal energy of meniscus formation
V	volume of liquid forming the meniscus
V_s	volume excess of meniscus state over bulk liquid state
V_e	excluded volume: volume of vapour in a volume-limited r.i.f.s. meniscus bounded by the cylinder of the dish perimeter and the horizontal plane of the rod
V_v	volume of vapour in the closed system of figure 1
W	work performed on the system to form a meniscus
X	horizontal coordinate or radius of tip or plate supporting a meniscus
X_d	radius of a circular dish in an r.i.f.s. system
X_0	radius of an orifice
Z	vertical co-ordinate or meniscus height
Z_0	height of apex of meniscus from free surface
Z_t	$(Z_0 - Z)$ height of free surface from supporting surface
Zg	height of supporting surface from centre of gravity of the meniscus

PHILOSOPHICAL TRANSACTIONS OF THE ROYAL SOCIETY A MATHEMATICAL, PHYSICAL & ENGINEERING SCIENCES

β	shape factor $\rho g b^2/\gamma$
β'	shape factor of r.i.f.s. menisci $\rho g R_h^2(270°)/\gamma$
γ	surface tension of liquid–vapour interface
γ_{I}	specific free energy of solid–liquid interface
γ_{s}	specific free energy of solid–vapour interface
θ	angle of contact defined by equation (2)
ρ	density difference between the liquid and its vapour
ϕ	meniscus angle: angle between principal radius and vertical axis of symmetry
π	3.14159

PHILOSOPHICAL TRANSACTIONS OF THE ROYAL SOCIETY A MATHEMATICAL, PHYSICAL & ENGINEERING SCIENCES